MONTHLY WEATHER REVIEW

VOLUME 79 NUMBER 7

JULY 1951

CONTENTS

U. S. DEPARTMENT OF COMMERCE · WEATHER BUREAU

CORRECTION

MONTHLY WEATHER REVIEW, June 1951, vol. 79, No. 6, cover: In contents, title of article by R. C. Schmidt should read "A Method of Forecasting Precipitation 28–40 Hours in Advance During October", instead of ". . . 24–40 Hours in Advance . . . ."

Page 123: In Table 2, lower left section, last heading on right should read "Total" instead of "Rain".

DEPARTMENT OF COMMERCE
CHARLES SAWYER, Secretary

WEATHER BUREAU
F. W. REICHELDERFER, Chief

MONTHLY WEATHER REVIEW

Editor, JAMES E. CASKEY, JR.

Volume 79
Number 7

JULY 1951

Closed September 15, 1951
Issued October 15, 1951

ON FORECASTING CEILING LOWERING DURING CONTINUOUS RAIN

LOUIS GOLDMAN

U. S. Weather Bureau Airport Station, Boston, Mass.

[Original manuscript received November 2, 1949; revised manuscript received April 13, 1951]

ABSTRACT

During steady rain, the ceiling lowers in a discontinuous fashion. The ceiling heights may be predicted with sufficient accuracy by using a set of empirically determined rules. To obtain a relation for the time of occurrence of these ceilings, the factors which influence cloud formation are considered. An expression is derived for the rate of moisture increase due to evaporation from falling raindrops. The rate of moisture change, given by this expression, is combined with the effect of the other factors in order to obtain a formula which may be applied to find the time a ceiling of given height will occur. The variables in the forecast formula are (1) the wet-bulb temperature depression measured before the start of rain and (2) F_s, the effective rate of moisture increase caused by factors other than evaporation. Values for F_s are found empirically. An approximate method, based on the surface value of the depression, is used for finding the time of occurrence of the 800-, 500-, and 300-foot ceilings. This approximate method appears to be best suited for forecasting the 500-foot ceiling.

CONTENTS

INTRODUCTION

Low ceilings [1] associated with rain occurring in advance of warm fronts or well-developed cyclones frequently restrict flying over a wide area. At times the ceiling becomes low at the time rain starts, while at other times the weather may be flyable for several more hours. In either case low ceilings occur in a large area at about the same time, making it difficult for the pilot caught in this weather to find a suitable landing place.

Findeisen [1] considered the problem and derived a formula for the rate of downward growth of the fracto-cumuli forming underneath the rain cloud during steady precipitation. His derivation is based on the assumption that all rain forms by the melting of snow falling out of the nimbostratus, accompanied by cooling of the air just beneath the cloud. This cooling causes a steepening of the temperature gradient below the zero isothermal, consequently increasing convection which results in the formation of the fracto-cumuli. Assuming that the heat required to melt all the precipitation comes from the surrounding air, Findeisen shows that the rate of downward growth of the low cloud is given by:

$$\frac{dc}{dt}=6.2N \qquad (1)$$

where N is the rate of rainfall in mm.hr.$^{-1}$ and dc/dt is the rate of lowering in cm.sec.$^{-1}$.

According to equation (1) clouds formed in rain lower at a rate directly proportional to the intensity of rainfall. An attempt to apply the result to forecast ceilings during

[1] The definition of the term "ceiling" is subject to change. In order that no confusion shall result, it will be employed here to mean the height, above the ground, of the base of the lowest cloud layer covering more than half the sky. This definition approximates the official meaning in effect at the time of the ceiling data used in this report. When no specification as to the amount of cloudiness is intended, terms such as "base height of cloud (or cloud layer)" or "height of base of cloud" will be employed.

964933—51——1

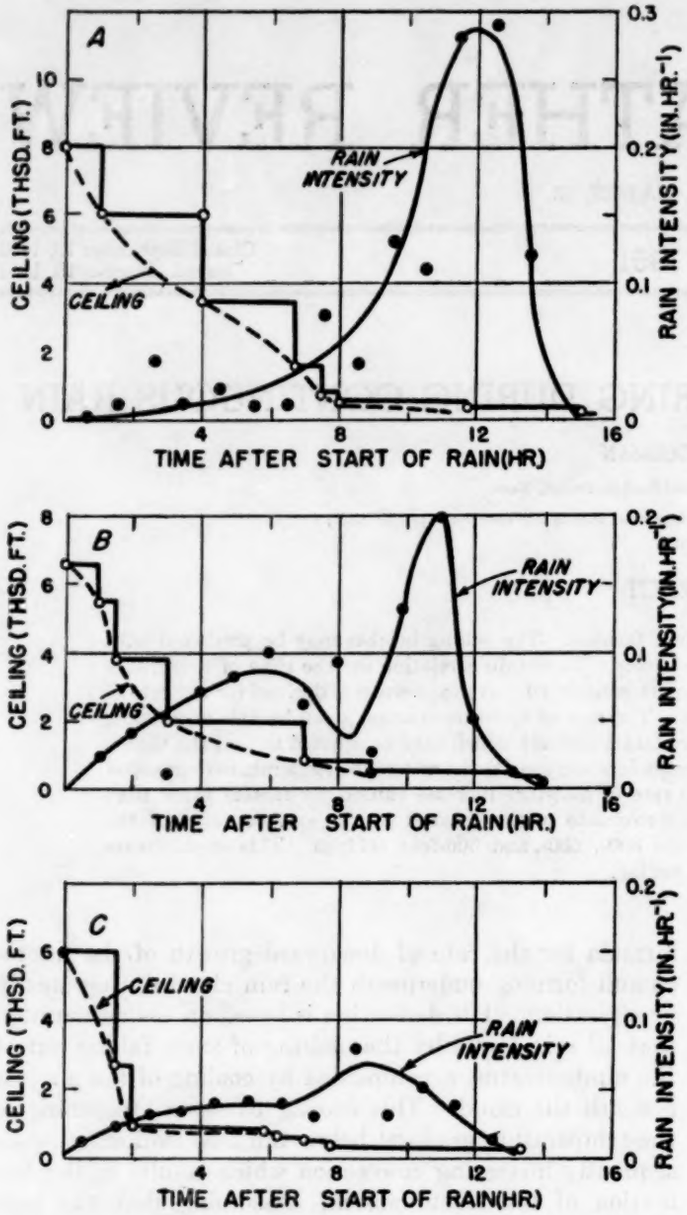

FIGURE 1.—Variation of ceiling and rain intensity in three typical cases observed at Boston. (A) April 24, 1944. (B) May 15, 1944. (C) March 7, 1948.

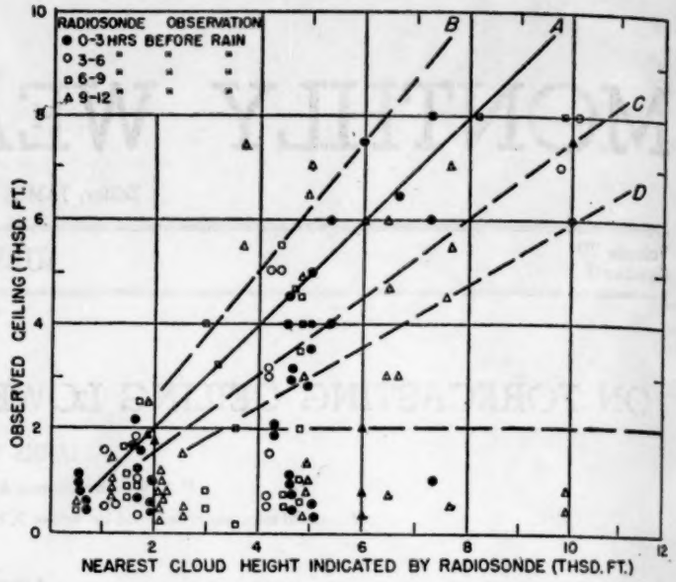

FIGURE 2.—Observed ceiling during rain plotted against the nearest level defined by rules (1) and (2) found from latest radiosonde preceding the rain. Portland, Maine, 1945–1947.

rain in eastern United States leads to failure, perhaps because conditions influencing cloud formation are somewhat different from those assumed by Findeisen.

Three typical cases of ceiling lowering during rain, observed at Boston, are shown in figure 1. The ceiling does not lower continuously, but appears to remain fixed until a cloud forms below this height and increases in amount sufficiently for its base height to become the ceiling. This ceiling then remains practically constant until another cloud layer, closer to the ground, appears and increases in amount so as to constitute the ceiling. In this manner the ceiling lowers discontinuously until a final cloud layer appears close to the ground. This final cloud layer may increase in amount and extend downward very slowly until the damp air is displaced by drier air.

The smoothed curves through the points representing ceiling and the corresponding time it was first observed are typical of those obtained for all cases and may be taken to define the variation of ceiling during continuous rain. Comparing the ceiling and rain intensity, it is seen that the ceiling lowers at a decreasing rate as the rain intensity increases, and that the minimum ceiling is reached before maximum rain intensity. Apparently the rate of ceiling lowering and rain intensity are negatively correlated.

With these observational facts in mind, it is the purpose of this study to examine rules which may be useful in forecasting variations of ceiling during rain, and, through a logical approach, to develop an objective method for predicting the rate of ceiling lowering during rain.

BASE HEIGHT OF CLOUD LAYERS DEVELOPING IN RAIN

Two generally well known rules are applied by the aviation forecaster to determine the base height of cloud layers likely to occur during rain. These are:

(1) The base of a cloud layer will be at a height where the temperature lapse rate changes from positive to less positive or negative.

(2) The base of a cloud layer will be at a height where the wet-bulb temperature depression, or dew point temperature depression, is a minimum.

To test these rules the Portland, Maine, surface reports for the years 1945, 1946, and 1947 were examined for all cases of continuous rain. All the differing ceilings reported during each rain period and all the heights defined by rules (1) and (2) found from the latest radiosonde preceding the

rain were listed. In a few cases where multiple heights were indicated within a short distance, the lowest height was selected. Due to an incomplete file of radiosonde data available, several cases were omitted, leaving a total of 32 cases for study. All the ceilings reported in these cases are shown plotted against the nearest height given by the radiosonde in figure 2. If the two rules gave both the necessary and sufficient conditions for determining the height of cloud bases, all the points in figure 2 would fall near the straight line OA. However, all the points do not fall near OA, and if the rules are still considered sufficient, then the deviations must be due to (1) errors in measuring or estimating the ceiling, (2) time lag from the radiosonde observation to the time of ceiling observation, or (3) continuous lowering of ceiling. The points above OA, of course, can not be in error because of continuous lowering. The greatest deviations occur in the points above OB, determined from radiosonde data preceding the rain by more than 9 hours; it is likely that a stratum of higher temperature or humidity appeared at these levels in the meantime. The smaller deviations included between OA and OB relate to cases with little or no lag in observation time and can be attributed to the unavoidable error of estimating or measuring the ceiling. Since the error of estimate is as likely to be positive as to be negative, all the points included between lines OB and OC may be considered to agree with the rules for forecasting the height of cloud bases and, in particular, the ceiling during steady rain.

A relatively large number of points fall near or below 1,000 feet. Since there is a large separation between these points and the clouds above them, it is unlikely that the points correspond to ceilings which lowered continuously. Furthermore, the error in the measurement of the base height of low clouds is generally negligible. These ceilings are reported regardless of the time lag between radiosonde observation and start of rain, so it must be assumed that a temperature inversion develops near the surface after the start of rain, if not sooner. The wind almost always increases with the approach of continuous rain. Mechanical turbulence associated with the increasing wind results in a temperature inversion not far from the ground. A maximum relative humidity at the base of the mechanically produced inversion and the inversion itself may not be evident in a radiosonde taken before the start of rain. Strong winds result in higher inversions and a more rapid development of the inversion so that the number of ceilings between 1,000 and 2,000 feet not associated with an inversion is smaller than the number below 1,000 feet.

If the few cases lying between line OD and the 2,000-foot level are attributed to a lag in observations, then the ceilings falling between OC and OD may be due to downward growth of a cloud base. However, most of these points are close to, or above, OC, so considering the possible error in observing ceilings, the continuous lowering of ceiling during rain is negligible in most cases.

This leads to the following additional rules which may be found useful in forecasting the variation of ceiling during rain:

(3) If the rain is of sufficient duration, a ceiling will occur below 2,000 feet. Most frequently it is a ceiling of 800 feet.

(4) During continuous rain a ceiling generally does not occur at the height of temperature discontinuity and/or maximum humidity until after the occurrence of a ceiling corresponding to the next higher level of temperature discontinuity and/or maximum humidity.

(5) The ceiling remains practically constant until the next lower cloud layer appears and increases sufficiently for its base height to become the ceiling.

Applying the above rules to available radiosonde data leads to a reasonably accurate forecast of the ceilings which will occur during continuous rain. From the study of ceiling variation it is obvious that if the radiosonde observation is taken over 6 hours before the start of rain then a significant ceiling may occur which is not given by the rules. However, whether or not such a ceiling can occur may be determined readily by inspection of radiosonde data closer to the rain area, or if these are not available, by noting the base heights of clouds reported in the rain area.

Since the ceilings which occur, when the rain is of sufficient duration, can be found with the degree of accuracy required in an aviation forecast, it remains to develop a method of forecasting the time these ceilings will first occur.

FACTORS INFLUENCING TIME OF CLOUD FORMATION

From the manner in which the ceiling varies during continuous rain, it appears that the important factors influencing the variation may be:

(1) *Advection of warmer and more humid air at selected levels.* In these strata of warm humid air which appear in advance of the rain area, the relative humidity increases upstream, reaching the 100 percent value at the forward edge of the cloud sheet. The cloud itself may not move at the speed of the wind because other factors associated with the rain tend to increase the relative humidity of the air in the strata.

(2) *Vertical mixing.* Mechanical turbulence at the boundary between the warm stratum and the colder air beneath it and in the layer next to the ground causes vertical mixing which tends to increase the moisture content of the upper part of the mixed layer at the expense of the lower part. If the moisture content of the mixed layer is sufficiently high, a cloud will form near the top of the mixed layer, as shown by Petterssen [2]. The base height of this cloud will remain constant until the moisture content, due to other factors (e. g., evaporation and advection), increases sufficiently to lower the mixing condensation level (MCL). Thus, if successively lower layers

form in intervals of a few hours, the gradual lowering of the cloud basis, except the lowest, is negligible when the ceiling variation is considered.

(3) *Evaporation from falling raindrops.* Evaporation is effective in increasing the relative humidity of the entire air column. The rate of evaporation is greater when the dryness of the air is greater. Evaporation moistens the dry air between the moist strata rapidly, but evaporation diminishes as the relative humidity increases, and unless the rain is warmer than the wet-bulb temperature of the surrounding air, evaporation alone cannot produce condensation. When the air is very dry in the lower layer, evaporation determines the time of formation of the lowest clouds. Vertical mixing may produce an inversion near the ground, but if the air is dry, the MCL will lie above the layer of mixing and no cloud will form; however, evaporation will increase the amount of moisture rapidly—the drier the air, the more rapid the increase. Eventually the MCL falls within the layer of mixing and a cloud forms near the base of the turbulence inversion. This cloud builds downward as evaporation continues.

The problem of determining the time it would take for a cloud to form due to the combined effect of advection, vertical mixing, evaporation and, perhaps, other factors is a complex one. However the problem may be simplified by confining attention to evaporation and allowing for the other factors by inclusion of a suitable parameter. Since the effects of vertical mixing and advection are highly correlated, each depending on the wind and moisture distribution surrounding the rain area, a single parameter may suffice for the effects of the two.

MOISTURE INCREASE DUE TO EVAPORATION

If a falling raindrop is conceived to be surrounded by a thin viscous air film, through which heat is transferred by conduction, and this boundary layer to be surrounded by a turbulent zone, through which heat is transferred convectively, then a relation for the transfer of heat between the raindrop and the surrounding free air may be derived readily. Thus, Newton's Law, which is applicable to the boundary layer, may be written:

$$\frac{dQ}{dt}=h_f a(T_b-T_r) \tag{2}$$

where dQ/dt is the rate of heat transfer through the film, a is the mean area of the film (which may be taken to be the surface area of the drop), T_r is the surface temperature of the raindrop and T_b is the temperature at the outer boundary of the air film. The heat conductance h_f is defined by the ratio k/δ, k being the conductivity of the film (which may be taken to be that for air) and δ the thickness of the film.

Taking equation (2) to define the "film" conductance of heat h_f, analogous equations are written to define the "convective" and "over-all" conductances, h_c and h_g, respectively, thus:

$$\frac{dQ}{dt}=h_c a(T-T_b) \tag{3}$$

and

$$\frac{dQ}{dt}=h_g a(T-T_r) \tag{4}$$

where T is the temperature of the free air.

If there is a continuous flow of heat between the raindrop and the free air, then $1/h_g=1/h_f+1/h_c$. By considering the dimensions of the variables upon which h_c and δ depend, i. e., the raindrop diameter d, its speed relative to the air v, the air viscosity μ, and the air density ρ, it can be shown that:

$$\frac{h_g d}{k}=\text{function of}\left(\frac{d v \rho}{\mu}\right)\equiv\phi(R)$$

where $R\equiv\frac{d v \rho}{\mu}$ is, by definition, the Reynolds Number for the raindrop. The form of the function ϕ may be found experimentally; however, except for a shape factor, which will be assumed to have the value of unity, the function may be approximated by the empirical relation:

$$\frac{h_g d}{k}=0.45+0.33(R)^{0.56} \tag{5}$$

which is based on the correlation of data for the flow of air at right angles to the axes of single cylinders ranging in diameter from 0.001 to 0.375 inch [3]. Values of h_g for the range of sizes found in rain, computed by equation (5) and based on R values calculated by Gunn and Kinzer [4] and $k=0.0000568$ cal. cm.$^{-1}$ sec.$^{-1}$(°C)$^{-1}$ are listed in table 1. For sizes ranging from 0.05 to 0.50 cm. there is only a 12 percent variation of individual values from the mean value of 0.0042 c. g. s. units so it may be assumed that h_g is constant for all raindrops.

TABLE 1.—*Terminal velocity, Reynolds number and over-all heat conductance for raindrops of various size*

d*	v†	R‡	h_g
Cm.	*Cm. sec.*$^{-1}$		*Cal. sec.*$^{-1}$ *cm.*$^{-2}$ *deg.*$^{-1}$
0.05	206	68.7	0.0046
.10	403	269	.0046
.15	541	542	.0045
.20	649	866	.0043
.25	742	1239	.0041
.30	806	1613	.0041
.35	852	1991	.0038
.40	883	2357	.0037
.45	900	2704	.0037
.50	909	3033	.0037

*Equivalent drop diameter calculated from the mass (Gunn and Kinzer [4]).
†Terminal velocity of fall for distilled water droplets in stagnant air at a pressure of 760 mm., temperature 20° C. and relative humidity of 50 percent (Gunn and Kinzer [4]).
‡Reynolds number = (air density) × (equivalent diameter) × (measured velocity) ÷ (viscosity of air). (Gunn and Kinzer [4].)

Now, if it is supposed that the heat required to evaporate rain comes from the surrounding air and that a state of equilibrium is reached instantaneously, then the tempera-

ture change dT, of a unit mass of air in the time interval dt, is

$$dT=-\frac{h_g A}{c_p}(T-T_w)dt \tag{6}$$

where T_w is the wet-bulb temperature, c_p the specific heat for air at constant pressure, and A the total raindrop area in unit mass of air. Neglecting variations in c_p, it remains to find the variation in A, in order to solve equation (6).

Lenard [5] measured the drop distributions in various types of rain and expressed the measurements in terms of the number of drops of each size falling on a unit horizontal area in a unit time. Using these data, the value of A near the ground may be computed from:

$$A=\frac{\pi}{\rho}\Sigma\left(\frac{n_i d_i^2}{v_i}\right) \tag{7}$$

where n_i is the number of drops of size d_i and terminal velocity v_i falling on a unit horizontal area in unit time. Values of A computed from this equation, together with a description of the rain and its intensity, as given by Lenard, are shown in table 2.

TABLE 2.—*Character of rain and surface area of raindrops*

Intensity	A	Character of rain
Mm. min.$^{-1}$	*Cm.*^{2} *gm.*$^{-1}$	
(1) 0.09	0.0083	Very ordinary looking rain.
(2) .06	.0097	Do.
(3) .11	.0058	Breaks occurred during which the sun shone.
(4) .05	.0045	Beginning of a thundershower.
(5) .32	.0115	Sudden rain from a small cloud.
(6) .72	.0292	Violent rain, like a cloudburst, some hail.
(7) .57	.0220	Heaviest period, less heavy period, and period
(8) .34	.0230	of stopping of a continuous fall which at times
(9) .26	.0085	took the form of a cloudburst.

There is a good correlation between the rain intensity and A, however the intensity values given by Lenard appear to be computed from the size distribution, which may account for this good correlation. To find the true relation between rain intensity and A, it is necessary to have data for measured rain intensity. These data are not available, so the type of rain will be considered instead.

At the beginning of rain, when the air is relatively dry, as in cases (3) and (4), A has a value from 0.004 to 0.006 cm^2gm^{-1}. The values increase to about 0.008 or 0.010 after the rain becomes steady, as in cases (1) and (2), and then remains at that value until stopping, case (9); but during rain of cloudburst intensity A may reach as high as 0.03 cm^2gm^{-1}. Since the minimum ceiling is generally observed to occur before the rain has reached its maximum intensity, it seems reasonable to assume A has the constant average value 0.005.

Equation (6) may now be solved readily to give:

$$\frac{\tau}{\tau_0}\equiv\frac{(T-T_w)}{(T-T_w)_0}=e^{-wt} \tag{8}$$

where $w\equiv\frac{h_g A}{c_p}$

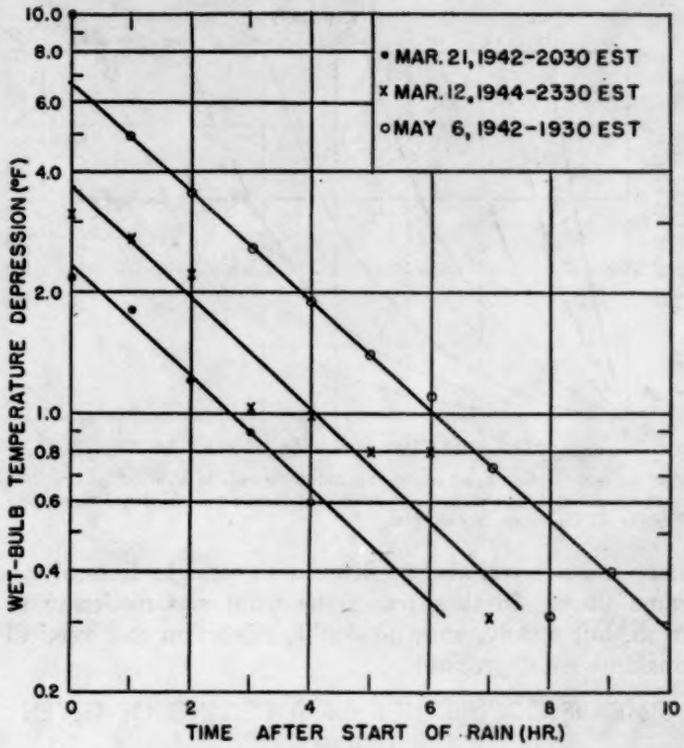

FIGURE 3.—Wet-bulb depression plotted against hours of rain for three cases of continuous rain at Boston, Mass.

and $\tau_0\equiv(T-T_w)_0$ is the value of the wet-bulb depression measured at the start and $\tau\equiv(T-T_w)$ is the value at the end of the time interval t.

Using the values found for A and h_g, and $c_p=0.24$ cal.gm.$^{-1}$ gives:

$$w=(0.0042)\ (0.005)\ (3600)/(0.24)=0.3\ \text{hr.}^{-1}$$

If factors other than evaporation may be neglected, then w may be computed directly from equation (8). These factors may be assumed negligible when the air is dry at the start of rain and the wind is light during the rain. However surface variations of depression only are available and, since the diurnal variation at the surface may be appreciable, the diurnal factors would have to be considered. The normal diurnal variation of the wet-bulb depression shows an almost constant value during the night, so to determine w from the surface variation it is best to select cases in which rain began during late evening.

A case in which evaporation appears to be the factor controlling the wet-bulb temperature depression occurred at Boston on May 6, 1942. Rain began at 1930 EST. The wind was SSW 15 to 20 m. p. h. until 2 hours before the start of rain when it diminished to less than 10 m. p. h. and then remained gentle for the remainder of the night. The wet-bulb depression plotted against hours of rain on semilogarithmic paper (fig. 3) gives a straight line of slope 0.30 hr^{-1}, thus verifying equation (8) and the value for w found indirectly. Two other cases plotted in the

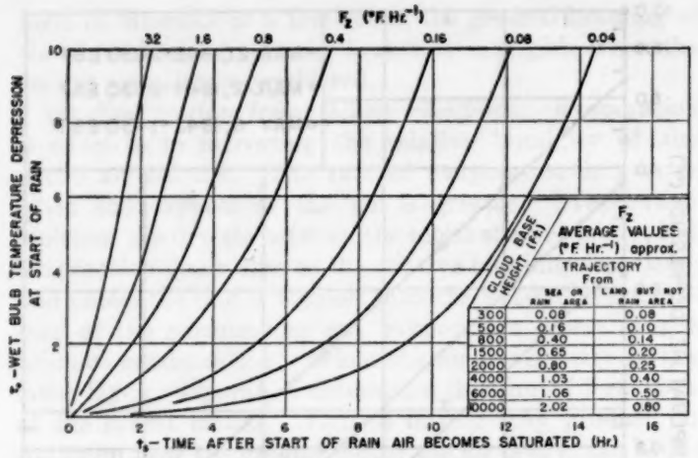

FIGURE 4.—Nomograph based on equation (10) giving t_s as a function of F_z and τ_0. The average values of F_z given in the table were determined from Portland, Maine, data using equation (12) or (13) (see fig. 5).

same manner can also be fitted with straight lines of the same slope. In these cases the wind was moderate to fresh, but steady, and, no doubt, advection and vertical mixing were appreciable.

TIME OF OCCURRENCE OF A CEILING OF GIVEN HEIGHT

If rain is at its equilibrium temperature then, according to equation (8), evaporation alone can not result in the formation of a cloud, since $t=\infty$ when $\tau=0$. However evaporation results in an exponential decrease in the depression, so it may well determine the time of cloud development, at least at times when the air is relatively dry at the start of rain.

Suppose factors, other than evaporation, cause an independent decrease in the wet-bulb temperature depression, say F_z per unit time, then the total rate of change of the depression during rain is

$$\frac{d\tau}{dt}=-(w\tau+F_z) \tag{9}$$

If it is assumed that F_z varies with height only, then the time t_s, after the start of rain, when the air at a given height becomes saturated is

$$t_s=\frac{1}{w}\log_e\left(1+\frac{w}{F_z}\tau_0\right) \tag{10}$$

where τ_0 is the value of the depression at that height at the time rain begins. Equation (10) is represented graphically in figure 4.

If the depression is measured t' hours before rain starts and has a value τ' at that time, then since F_z has been assumed constant, the depression at the start of rain is

$$\tau_0=\tau'-F_z t' \tag{11}$$

which may be subsitiuted in equation (10) to find t_s. However, if $\tau'<F_z t'$, then the time of saturation, t'_s, in hours after the time τ' is measured is simply:

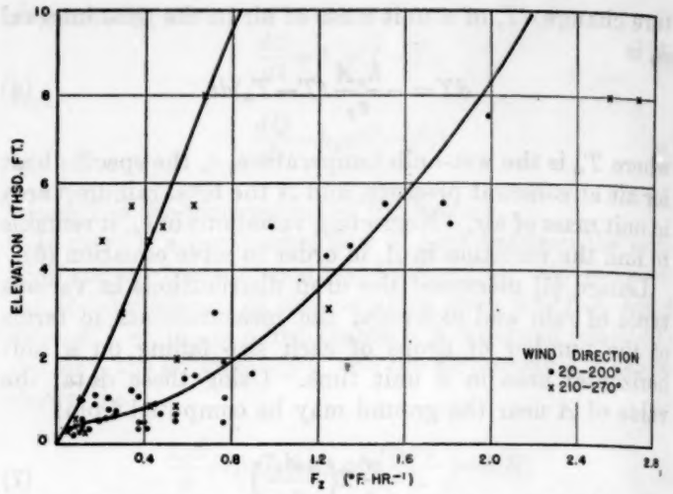

FIGURE 5.—Values of F_z by elevation determined from Portland, Maine, data using equation (12) or (13).

$$t'_s=\frac{\tau'}{F_z} \tag{12}$$

Obviously use of equations (11) and (12) will underestimate the time of saturation; the error will be greatest when τ' is measured long before the start of rain, i. e., before F_z becomes constant. In most cases F_z can not be determined directly, so it will be considered sufficient for this study to obtain some empirical values suitable for forecasting the time a ceiling of given height will occur. Such values may be computed readily from a combination of equations (10) and (11), i.e.,

$$F_z=\frac{\tau'}{t'+\frac{1}{w}(e^{wt_s}-1)} \tag{13}$$

or from equation (12), when the time of saturation is close to the time rain begins. Now, if the time a ceiling of given height first occurs is taken for t_s (or t'_s) then the values for F_z determined by using equations (12) or (13) may be considered appropriate corrected values for finding the time a ceiling of given height will occur.

Such values of F_z were found from the Portland, Maine data and are shown plotted in figure 5. Evidently the points fall in two classes; in one, F_z is relatively large, and in the other it is small. From the winds aloft last reported near the start of rain, it was found that the smaller set is associated with winds having a direction of 210° to 270°, and the larger set of values associated with a wind direction of 20° to 200°—except for a few cases.

It appears that the higher values correspond to cases in which the air trajectory passes either over water or close to the center of the rain area; while the lower values correspond to cases in which the air has a land trajectory not passing close to the rain area center. For places on the North Atlantic Seaboard, such as Portland and Boston, when continuous rain is associated with secondary Lows traveling northward, the higher F_z values should generally be applicable. The smoothed values given in figure 4 are

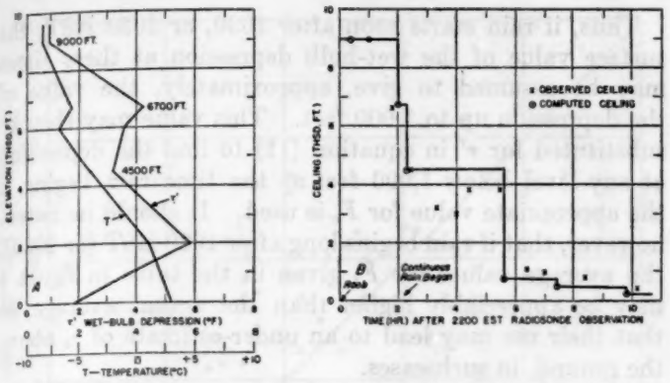

FIGURE 6.—(A) Temperature (T) and wet-bulb temperature depression (T') from Portland, Maine, sounding, 2200 EST, April 10, 1946. (B) Comparison of computed with observed ceiling at Portland, Maine, April 10-11, 1946.

based on insufficient data to be considered very reliable, however they may be used until better estimates are made. To illustrate the application of the results obtained so far, we now consider an example forecast of ceiling during continuous rain based on upper air data.

EXAMPLE OF USE OF UPPER AIR DATA TO FORECAST CEILING DURING RAIN

Rain began at Portland 0015 EST, April 10, 1946. The lapse rates of temperature and wet-bulb temperature, as determined from the 2200 EST radiosonde of the 9th, are shown in figure 6. At 2300 EST, the pibal reached 9,000 feet, indicating winds of 150° to 210° at all levels. With these data, the forecast of ceiling is made as follows:

The temperature and depression lapse rates indicate that ceilings of (a) 9,000 feet, (b) 6,700 feet, and (c) 4,500 feet will occur if the rain is of sufficient duration. Ceilings of less than 4,500 feet are not indicated, therefore the other heights selected are (d) 800 feet, (e) 500 feet, and (f) 300 feet. The 800-foot ceiling height is selected because it has been found to be the most frequent low ceiling. The 500- and 300-foot ceilings are chosen for their significance to aviation.

Considering each ceiling in turn:

(a) *9,000 feet.*

From the depression lapse rate, $\tau'=0.9°$ F.

From the table in figure 4, $F_z=2.1°$ F. hr^{-1}.

Since $F_z t'=(2.1)\ (2.25)>\tau'$, equation (12) is applied: $t'_s=\tau'/F_z=0.4$ hrs. after the observation of τ', i. e., the 9000-foot ceiling will occur at *2224 EST.*

(b) *6,700 feet.*

From the depression lapse rate, $\tau'=3.6°$ F.

From the table in figure 4, $F_z=1.7°$ F. hr^{-1}.

$F_z t'=(1.7)\ (2.25)=3.8>\tau'$, so $t'_s=3.6/1.7=2.1$ hrs. after 2200 EST, or at *0006 EST.*

(c) *4,500 feet.*

$\tau'=3.2$, $F_z=1.4$; $F_z t'=3.2=\tau'$; therefore the 4,500-foot ceiling occurs at the time rain starts, i. e., at *0015 EST.*

(d) *800 feet.*

$\tau'=3.5$, $F_z=0.4$; $F_z t'=0.9<\tau'$; therefore applying equation (11): $\tau_0=\tau'-F_z t'=2.6$.

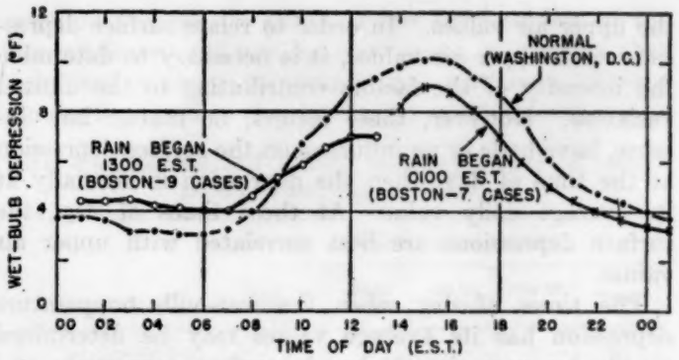

FIGURE 7.—Diurnal variation of wet-bulb temperature depression.

From figure 4, for $\tau_0=2.6$ and $F_z=0.4$, it is found that $t_s=3.5$ hrs., i. e., an 800-foot ceiling will occur 3.5 hrs. after the start of rain, or at *0345 EST.*

(e) *500 feet.*

$\tau'=2.8$, $F_z=0.16$, $\tau_0=2.4$, $t_s=5.7$ hrs. after rain starts, i. e., at *0600 EST.*

(f) *300 feet.*

$\tau'=2.4$, $F_z=0.08$, $\tau_0=2.2$, and $t_s=7.4$ hrs. after rain starts, or at *0745 EST.*

A comparison of this computed variation of ceiling with the actual ceiling variation is shown in figure 6.

ESTIMATE OF WET-BULB DEPRESSION IN LOWER LAYERS FROM SURFACE VALUES

Moisture gradients in the lower levels are usually variable in advance of rain, and since radiosonde data are relatively scarce, it is desirable to make use of surface data to predict the time of occurrence of low ceilings. It has been mentioned that the diurnal variation of the surface depression may be appreciable and should be considered. Surface values before the start of rain may not be a good measure of the value a few hundred feet from the ground, where the diurnal factors may be less important.

Generally, the range of the diurnal variation increases with the dryness of the air, so there should be very little diurnal variation during rain. However, near or before the start of rain, diurnal factors may cause a large variation. Thus, comparing the depression variation before the start of rain with the normal daily variation in figure 7, it is seen when rain begins in the early afternoon, the depression increases its value by about 75 percent from early morning to near noon; when rain begins near midnight, the depression lowers during the afternoon and evening at a rate not very different from the normal lowering.

A rough measure of the depression above the layer of diurnal influence may be made by assuming that the actual variation is proportional to the normal and applying a correction to the surface depression depending upon the time of day. These correction factors would, however, be unreliable when applied to depressions measured at night because there is very little correlation between the minimum surface depression reached at night and

the upper air values. In order to relate surface depressions with upper air values, it is necessary to determine the intensity of the factors contributing to the diurnal variation. However, these factors, no matter how intense, have little or no influence on the surface depression at the time of day when the depression is normally at its average daily value. At these times of day, the surface depressions are best correlated with upper air values.

The times of day when the wet-bulb temperature depression has its average values may be determined readily by averaging 24 hourly surface depressions and finding the time of day this average occurs on the smoothed diurnal variation. Approximate average values obtained in this manner, but by using the difference between average hourly temperature and wet-bulb temperature values [6] for Washington, D. C., are shown in table 3.

TABLE 3.—*Time of day wet-bulb depression has its daily average value, Washington, D. C. (Eastern Standard Time)*

Month	A. M.	P. M.	Month	A. M.	P. M.	Month	A. M.	P. M.
Jan	1030	2130	May	0930	2030	Sep	0900	1930
Feb	1100	2230	June	0930	2030	Oct	0930	2000
Mar	1000	2230	July	0930	2030	Nov	1030	2030
Apr	0930	2130	Aug	0930	2030	Dec	1030	2030
						Annual	1000	2030

Thus, the depression is normally at its mean value at 1000 EST and again at 2030 EST. Since upper air observations are made at about 1030 and again at 2230 EST, it follows that the morning radiosondes are best suited for finding the correlation of upper air depressions and surface values. This is made obvious in figure 8, which contains scatter diagrams relating the wet-bulb depressions at the surface, 500 feet, and 1,000 feet for both the morning and evening observations taken within 12 hours before the start of rain. Further, since the 1030 EST points in both diagrams fall reasonably close to a straight line of unity slope, the vertical gradient of the wet-bulb temperature depression below 1,000 feet before rain starts, is nearly zero at the times of day when diurnally varying factors do not contribute to the wet-bulb depression.

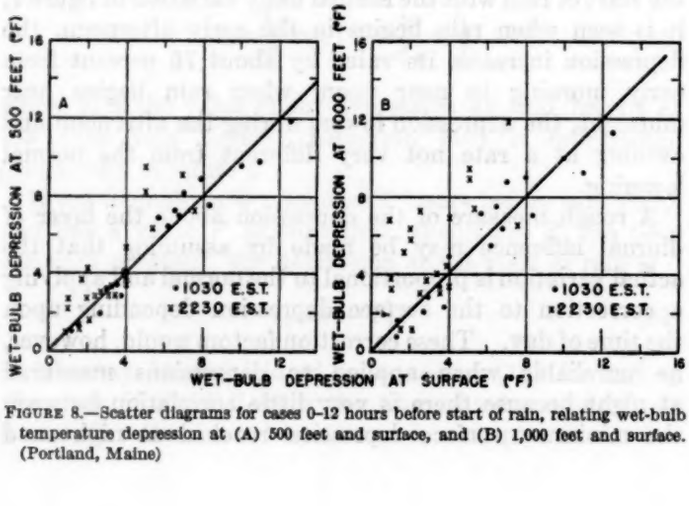

FIGURE 8.—Scatter diagrams for cases 0–12 hours before start of rain, relating wet-bulb temperature depression at (A) 500 feet and surface, and (B) 1,000 feet and surface. (Portland, Maine)

Thus, if rain starts soon after 1030, or 2030 EST, the surface value of the wet-bulb depression at these times may be assumed to give, approximately, the value of the depression up to 1,000 feet. This value may then be substituted for τ' in equation (11) to find the depression at any level below 1,000 feet at the time rain begins, if the appropriate value for F_z is used. It should be noted, however, that if rain begins long after 1030 EST (or 2030), the average values for $\bar{F}_z$ given in the table in figure 4 may be appreciably higher than the actual average, so that their use may lead to an under-estimate of τ_0 above the ground, in such cases.

FORECASTING TIME OF CEILING OCCURRENCE USING SURFACE WET-BULB DEPRESSION

To illustrate the application of surface elements measured before the start of rain to predict the time low ceilings will occur, the ceiling heights of (a) 800 feet, (b) 500 feet, and (c) 300 feet will be chosen for consideration. If the higher values for F_z are chosen from the table in figure 4, then equations (11) and (12), for each level become:

(a) *800 feet.* If $\tau' > 0.4t'$, then

$$\tau_0 = \tau' - 0.40t' \tag{11a}$$

where τ' is the surface wet-bulb depression measured at 1030 EST, or 2030 EST, whichever is closest to the time rain starts, and t' is the number of hours to the start of rain. The number of hours, after the start of rain, when the 800-foot ceiling will first occur can then be found from figure 4 using the value of τ_0 given by equation (11a) and the value $F_z = 0.40$.

If $\tau' \leq 0.4t'$, then the time the given low ceiling will first occur, in hours after the measurement of τ', is

$$t_s' = 2.5\tau' \tag{12a}$$

Similarly for the other levels:

(b) *500 feet.* If $\tau' > 0.16t'$, then

$$\tau_0 = \tau' - 0.16t' \tag{11b}$$

and if $\tau' \leq 0.16t'$, then

$$t_s' = 6.3\tau' \tag{12b}$$

(3) *300 feet.* If $\tau' > 0.08t'$, then

$$\tau_0 = \tau' - 0.08t' \tag{11c}$$

and if $\tau' \leq 0.08t'$, then

$$t_s' = 12.5\tau' \tag{12c}$$

These formulas, together with figure 4, were tested on all cases of continuous rain which occurred at Boston during the years 1944 and 1945, assuming that the values of $\bar{F}_z$ found for Portland apply. Cases in which low ceilings occurred before the start of rain were omitted. The average of the wet-bulb depressions measured at 0930, 1030, and 1130 EST (or 1930, 2030, and 2130 EST) was taken for τ', in order to reduce possible errors in the measurement of the depression. For cases in which rain began close to 1030 or 2030 EST, the last two measurements before the start of rain were averaged so that the later data could be used. In any case, the average time of the averaged measurements to the time of beginning of rain was used for t'. The resulting forecasts are compared

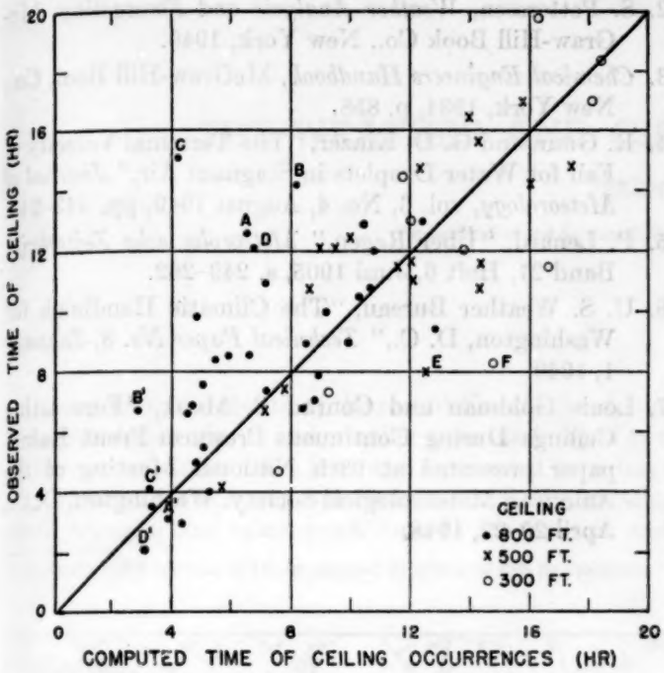

FIGURE 9.—Comparison of forecast with actual time of ceiling in rain at Boston, Mass., 1944 and 1945.

with the time that the ceiling was first reported, at or below the given height, in figure 9. In most cases the error is within 3 hours.

Points A, B, C, and D in figure 9 represent the only 800-foot cases for which t' is more than 8 hours. For all other cases t' is 8 hours or less. The large deviations in cases A, B, C, and D may be attributed to the error resulting from the application of the average F_s value over too great a time interval. If the surface values before the start of rain are used to give a better measure for the wet-bulb depression at 800 feet at the start of rain, the points A, B, C, D translate to A′, B′, C′, D′, respectively.

The two points E and F show the largest departure in the opposite direction. These correspond to a single case. Actually the ceiling lowered from 900 feet to 200 feet within 2 hours just ahead of a warm front, preceded by light winds and drizzle. It is to be expected that when a front lies in the vicinity of the station, before the time rain can produce low cloudiness, the properties of the front, with respect to low clouds and fog, determine the ceiling, and therefore should be considered in an actual forecast.

In many cases the ceiling did not lower to the selected levels, so not all the forecasts made appear in figure 9. To show how the formulas apply to all cases, the contingency table 4 was prepared. This table compares the lowest ceiling observed in each case with the minimum ceiling that would have been forecast if the time of ending of ceiling lowering was known; for example, the time dry air advection begins or the time rain ends. Since the computed minima are within a few hundred feet of the observed lowest ceilings, in most cases, it appears that conditions favoring saturation did not continue a sufficient time for the cloud to develop at the selected level.

TABLE 4.—*Computed and observed minimum ceiling in rain at Boston, Mass., 1944 and 1945*

		Number of cases forecast				
		Less than 400 feet	400 to 500 feet	600 to 800 feet	Over 800 feet	Total
Number cases observed	Less than 400 feet	7	2	1	0	10
	400 to 500 feet	3	5	1	0	9
	600 to 800 feet	1	4	5	1	11
	Over 800 feet	0	0	0	2	2
	Total	11	11	7	3	32

CONCLUSION

It is evident from this study that it is possible to predict the rate of ceiling lowering during rain, objectively and with a reasonable degree of accuracy. Although several important factors influencing cloud formation have either been neglected or roughly approximated in the derivation of the forecast method, a logical approach was attempted in order that the forecaster may at least make an approximate allowance for the effect of these factors, when known or extrapolated. The following list, although incomplete, suggests how forecasts made from figure 4 may be improved qualitatively by the forecaster and, of course, suggests the lines along which further study should be made in order to improve the accuracy of ceiling forecasts:

(1) If a front or trough, with which low ceilings are associated, lies nearby, then the ceiling may lower more rapidly than forecast.

(2) In cases of heavy rain or snow, near the beginning of precipitation, the ceiling will lower more rapidly than forecast.

(3) With strong turbulence near the ground the time of formation of very low clouds may be underestimated, while the time of formation of clouds near the top of the mixed layer may be overestimated.

(4) Ceilings may not lower as rapidly as forecast in cases of intermittent or showery precipitation.

(5) The time a ceiling of given height will occur may be underestimated if there is only slight advection of moist air at that level; if there is dry air advection, the ceiling may rise (e. g., near the time rain ends).

Perhaps the greatest improvement in forecasting the time of occurrence of the very low ceilings may be attained by (a) using F_s values indicated by wind and wet-bulb depression distributions, and (b) a study of frontal characteristics.

ACKNOWLEDGMENTS

The author wishes to acknowledge the encouragement and helpful advice given during the course of this study by Mr. C. F. Van Thullenar, Mr. Paul H. Kutschenreuter,

964933—51——2

and the members of the forecast staff at the Boston Weather Bureau Office. Special acknowledgment is due Mr. Conrad P. Mook, who presented parts of this paper with his study of ceiling lowering at Washington as a joint work before the American Meteorological Society [7]. Unfortunately, other commitments have prevented Mr. Mook from completing his report in time to be included with this paper.

REFERENCES

1. W. Findeisen, "Die Entstehung der 0°-Isothermie und die Fraktocumulus-Bildung unter Nimbostratus," *Meteorologische Zeitschrift*, Band 57, Heft 2, Februar 1940, s. 49–54. Translation by F. A. Berson, "The Formation of the 0°-isothermal Layer and Fractocumuli Under Nimbostratus," Meteorological Offices, London. Copy available in U. S. Weather Bureau Library.
2. S. Petterssen, *Weather Analysis and Forecasting*, McGraw-Hill Book Co., New York, 1940.
3. *Chemical Engineers Handbook*, McGraw-Hill Book Co., New York, 1934, p. 858.
4. R. Gunn and G. D. Kinzer, "The Terminal Velocity of Fall for Water Droplets in Stagnant Air," *Journal of Meteorology*, vol. 6, No. 4, August 1949, pp. 243–248.
5. P. Lenard, "Über Regen," *Meteorologische Zeitschrift*, Band 21, Heft 6, Juni 1905, s. 249–262.
6. U. S. Weather Bureau, "The Climatic Handbook for Washington, D. C.," *Technical Paper No. 8*, January 1, 1949.
7. Louis Goldman and Conrad P. Mook, "Forecasting Ceilings During Continuous Prewarm Front Rain," paper presented at 98th National Meeting of the American Meteorological Society, Washington, D. C., April 20–22, 1948.

THE WEATHER AND CIRCULATION OF JULY 1951[1]

VINCENT J. OLIVER

Extended Forecast Section, U. S. Weather Bureau, Washington, D. C.

During July, the month of the record Kansas flood, the mean circulation (fig. 1) and weather were made up of two contrasting regimes. The first was dominated by a huge ridge throughout the troposphere over the Gulf of Alaska which brought cool rainy conditions to the Central and Northern Plains States, while the weather continued warm and dry in the Far West and Deep South. The second was characterized by the opposite flow pattern with a trough off both coasts of the United States, a ridge in the center, and a markedly reversed precipitation pattern.

[1] See Charts I-XV following p. 152, for analyzed climatological data for the month.

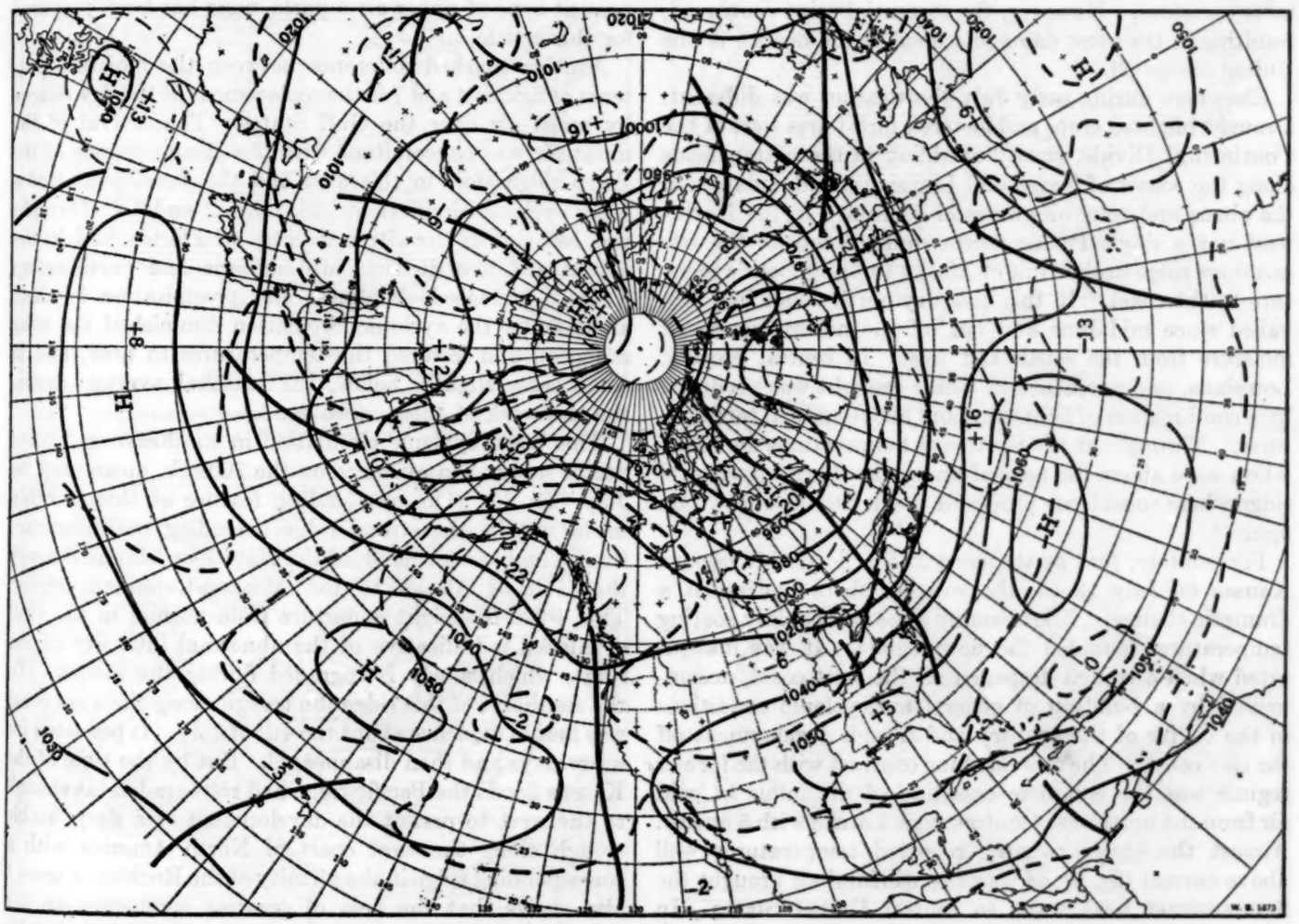

FIGURE 1.—Mean 700-mb. chart for the 30-day period June 30-July 29, 1951. Contours at 200-foot intervals are shown by solid lines, intermediate contours by lines with long dashes, and 700-mb. height departures from normal at 100-foot intervals by lines with short dashes with the zero isopleth heavier. Anomaly centers and contours are labeled in tens of feet. Minimum latitude trough locations are shown by heavy solid lines.

The first regime is illustrated in figures 2, 3, and 4. The strong 700-mb. ridge shown in figure 2 in Alaska and the Gulf of Alaska first became pronounced in western Canada in April and gradually retrograded to the position shown reaching its peak intensity in late June to early July [1]. East of it, and to the west of the unusually deep trough in east-central Canada, strong northerly winds poured cold air far down into the central United States. The southern edge of the cold air mass stagnated just south of Kansas. This is well indicated by the fact that temperatures for the week of July 10–17 averaged more than 3° F. above normal in Texas but more than 6° below normal in Nebraska (fig. 3). During this same period a pronounced current of moisture-laden air from the Gulf of Mexico (fig. 4) streamed northward into Kansas, up over the southern edge of the cold dome, and then continued eastward. This flow pattern brought copious rainfall to the central Plains where precipiatation had been above normal every month since February. By the end of June the soil there, already saturated, could absorb no more moisture. However, the torrential rains continued, resulting in the most damaging flood in the history of the United States [2].

Elsewhere during early July the weather was different. Drought blighted crops and fostered forest fires west of the Continental Divide, caused shedding in the cotton fields along the coasts of Texas and Louisiana, and endangered the citrus and tung oil groves of Florida. In the Northwest not a single Pacific storm could penetrate the tremendous ridge in the Gulf of Alaska to bring Pacific moisture to the coast. In this area dry north winds had prevailed since mid-June and cut off the normal source of moisture from the south and west. In central Florida, Louisiana, and northeastern Texas drought was produced by a combination of light rains and above-normal temperatures. Throughout the Southeast temperatures and insolation were above the normal under the sharp upper-level ridge where subsidence produced the dry tongue shown on figure 4.

Fortunately, just as the crest of the floods hit eastern Kansas on July 13–15, the weather there underwent a dramatic change. Bright sunny skies and rapidly soaring temperatures heralded the new regime. It was inaugurated when a trough deepened off the west coast, accompanied by a build-up of general anticyclonic conditions in the center of the country and trough development off the east coast. The most striking contrast with the former regime was the complete cessation of the influx of cold air from the northwest (contrast figs. 2 and 3 with 5 and 6). Almost the entire country reported temperatures well above normal (fig. 6), as warm continental air brought the first summer heat wave to central United States. In parts of the northern and central Plains States temperatures during the last week of July averaged more than 20° F. higher than they had been during the first week of the month.

The moisture pattern, like the temperature pattern, during the latter part of July was radically different from that characterizing the earlier weather regime, as can be seen by a comparison of figures 4 and 7. The extensive moist tongue from the Gulf of Mexico shifted westward, giving widespread showers to the parched Southwest. These were especially heavy in Utah and Nevada, where local flash floods occurred. As is evident from the temperature charts (figs. 3 and 6) these rains were not caused by the forced ascent of warm moist air over a cold air dome, as were the Kansas rains in the earlier regime. On the contrary, during the latter half of July the precipitation associated with the moist tongue was primarily convective and orographic in nature. A better representation of the three-dimensional moisture distribution could probably be obtained on an isentropic surface instead of on the 700-mb. surface. However, due to the difficulties of constructing isentropic charts from our present type of upper air reports, none has been prepared for this article.

Another marked difference between the moisture patterns of figures 4 and 7 is the replacement of the dry tongue by moist air over the Gulf States. The arrival of the moist air was concomitant with the disappearance of the sharp ridge aloft in this area and the development of a weak cyclonic circulation. (See figs. 2 and 5.) Drought was relieved in the citrus country of Florida and in the cotton and rice districts of Louisiana and northeastern Texas. Increased cloudiness and precipitation in these areas under the cyclonic circulation diminished the solar radiation and lowered the temperatures to near, and in some cases slightly below, the seasonal average during the last week of July. (See fig. 6.)

This weak cyclonic circulation in southeastern United States was not in evidence on the 700-mb. mean map for July (fig. 1). The outstanding feature of this monthly mean map is the strong ridge extending northeastward from a high center north of the Hawaiian Islands through the Gulf of Alaska to the Alaskan-Canadian border. The +220-ft. height departure from normal in the Gulf of Alaska is indicative of the abnormal intensity of the ridge, which slowly retrograded during the month. To the southeast of this ridge the trough along the west coast was first in evidence about the 4th of July. It persisted for a few days and then disappeared. But by the time of the Kansas floods the Pacific ridge had retrograded far enough to the west to permit the development of a deep, stable trough along the west coast of North America with a corresponding ridge in the vicinity of the Rockies. Figure 1 also shows that the area of greatest confluence on the monthly mean chart was located along the northern border of the United States. Rainfall generally exceeds the

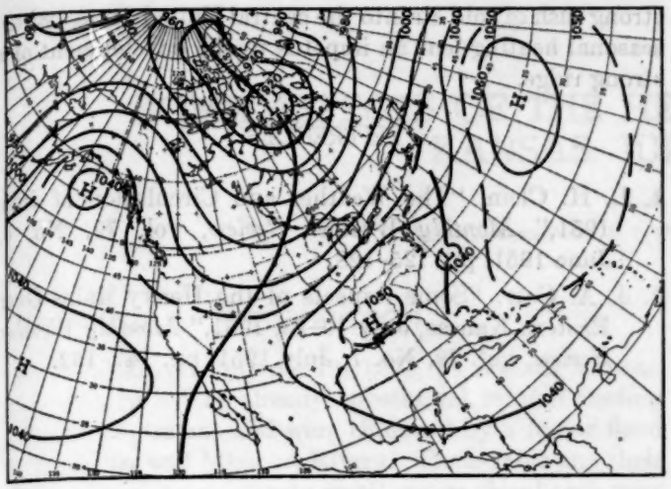

FIGURE 2.—Mean 700-mb. chart for the 5-day period July 7–11, 1951. Contours at 200-foot intervals are shown by solid lines, selected intermediate contours by dashed lines, and minimum latitude trough lines by heavy solid lines.

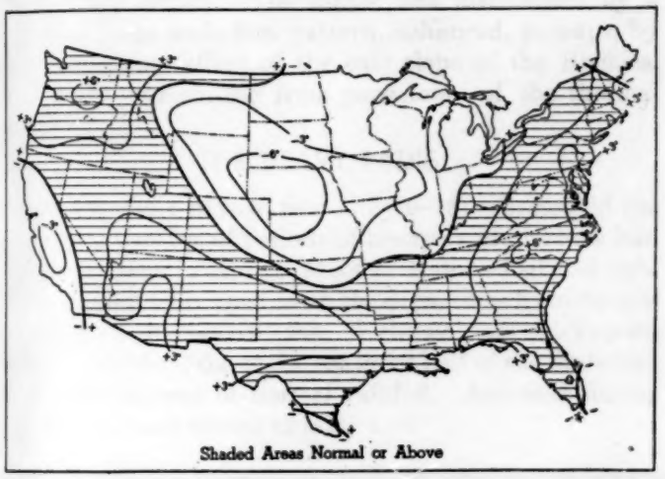

FIGURE 3.—Departure of mean temperature from normal for the week ending July 17, 1951. (From U. S. Weather Bureau, *Weekly Weather and Crop Bulletin*, week ending July 17, 1951.)

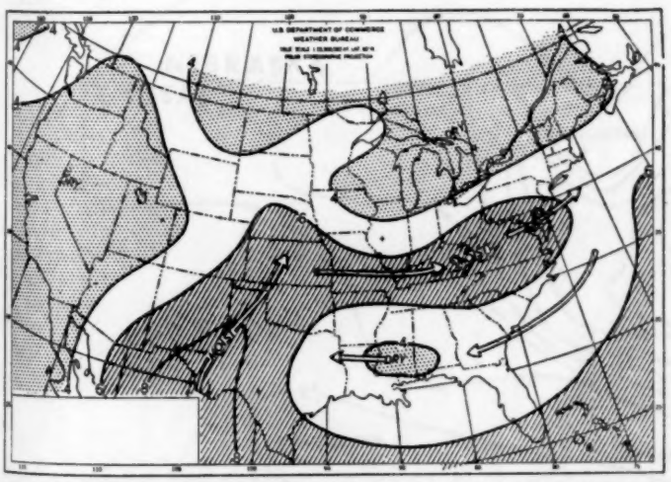

FIGURE 4.—Mean 700-mb. moisture chart for the 5-day period July 11–15, 1951. Areas with mixing ratio above 6 gm/kg of dry air are hatched. Areas with less then 4 gm/kg are dotted. Arrows indicate schematic flow of principal moist and dry tongues.

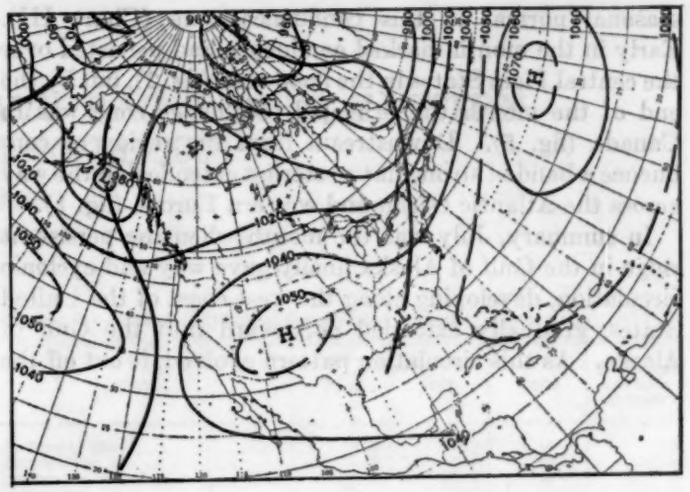

FIGURE 5.—Mean 700-mb. chart for the 5-day period July 28–August 1, 1951. Contours at 200-foot intervals are shown by solid lines, selected intermediate contours by dashed lines, and minimum latitude trough lines by heavy solid lines.

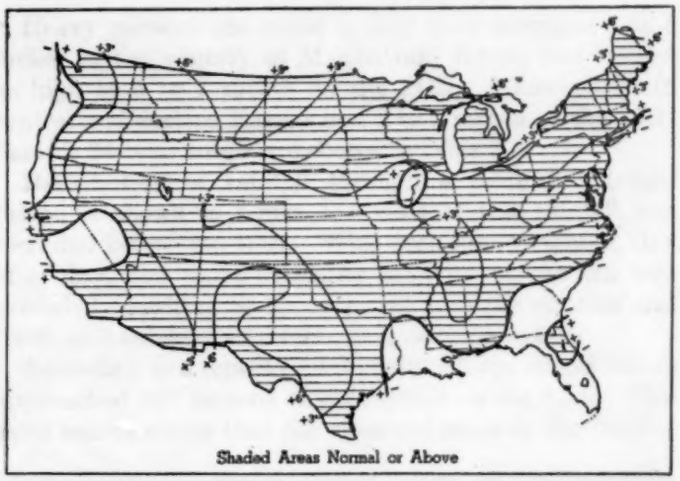

FIGURE 6.—Departure of mean temperature from normal for the week ending July 31, 1951. (From U. S. Weather Bureau, *Weekly Weather and Crop Bulletin*, week ending July 31, 1951.)

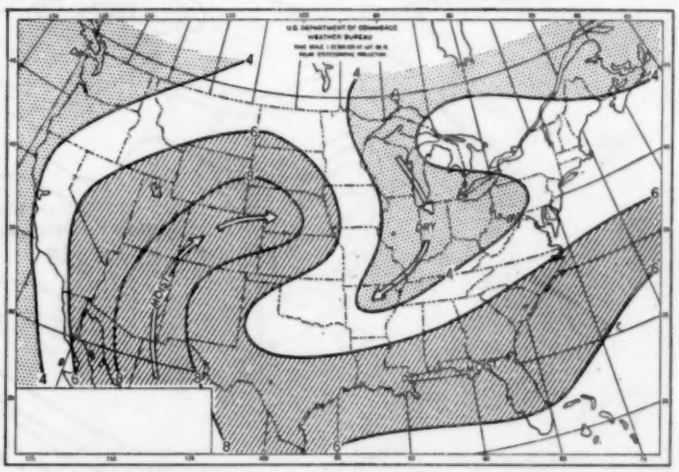

FIGURE 7.—Mean 700-mb. moisture chart for the 5-day period July 28–Aug. 1, 1951. Areas with mixing ratio above 6 gm/kg of dry air are hatched. Areas with less than 4 gm/kg are dotted. Arrows indicate schematic flow of principal moist and dry tongues.

seasonal normal in this confluence zone (Chart III). Early in the month marked confluence had persisted over the central Plain States in the flood area (fig. 2), but by the end of the month the principal confluence zone was in Canada (fig. 5). Downstream from the region of confluence a band of strong flat westerlies extended all the way across the Atlantic Ocean and western Europe (fig. 1).

In summary, July was the month when the persistent ridge in the Gulf of Alaska finally gave way and cyclonic circulation, developing along the west coast of the United States, gradually extended northward into the Gulf of Alaska. As this circulation pattern evolved, it cut off the strong rush of cold air into the central United States, where seasonal heating lent an impetus to the development of a strong ridge.

REFERENCES

1. L. H. Clem, "The Weather and Circulation of June 1951," *Monthly Weather Review*, vol. 79, No. 6, June 1951, pp. 125–128.
2. J. A. Carr, "Some Aspects of the Heavy Rains Over Eastern Kansas, July 10–13, 1951," *Monthly Weather Review*, vol. 79, No. 7, July 1951, pp. 147–152.

SOME ASPECTS OF THE HEAVY RAINS OVER EASTERN KANSAS, JULY 10–13, 1951

J. A. CARR

WBAN Analysis Center, U. S. Weather Bureau, Washington, D. C.

INTRODUCTION

Heavy rains on July 10–13, 1951, in eastern Kansas, followed a period of already substantial rainfall feeding into swollen streams and were climaxed by a major flood in the Kansas and Missouri Rivers. These rains and their persistence over a relatively small geographical area may be explained in terms of the slow movement of a synoptic situation that favored continued inflow and lifting of moist air over the region. The inflow was maintained by a particular large scale flow pattern, enhanced, perhaps, by some channeling effect of the east slope of the Rockies, and the lifting resulting from persistence of the thermal pattern.

THE HEAVY RAINS

Actually, the 4 days of rain (July 9–13) represented the climax to a number of periods of heavy rainfall which had their beginnings in April. Most of Kansas had had substantial amounts in April, with the departures from normal exceeding 2 inches in the Wichita-Goodland-Topeka triangle. In May, the entire southern half of the State had 100 to 200 percent of normal rainfall. Amounts during June and July are shown in table 1.

TABLE 1.—*Rainfall (inches) for selected stations, June–July, 1951 [1]*

Station	June	July	Total	Total days 0.01 inch or more
St. Joseph, Mo.	13.73	5.72	19.45	29
Kansas City, Mo.	8.42	7.54	15.96	29
Lecompton, Kans.	11.17	10.87	22.04	25
Manhattan, Kans.	11.12	15.32	26.44	30
Topeka, Kans.	10.81	11.01	21.82	28
Wamego, Kans.	12.47	10.45	22.92	28

Heavy rains on the night of July 9–10 averaged 4 to 5 inches in the vicinity of Manhattan, Kans., and ranged as high as 5 to 7 inches on the 11th. Many places in central and eastern Kansas had 2 to 5 inches on the 12th. Sample 24-hour totals are shown in table 2.

Distribution of rainfall through a somewhat longer period is shown in figure 1. Most of this rainfall was recorded before the 13th. With such heavy rainfall, day after day, the water retaining capacity of the soil was exceeded, resulting in heavy runoff into the streams and rivers and subsequent overflowing of their banks.

According to a report by Hundeby [1], the runoff values approached 100 percent of the rainfall on the 12th. This same source states that the observed stage in the Fairfax

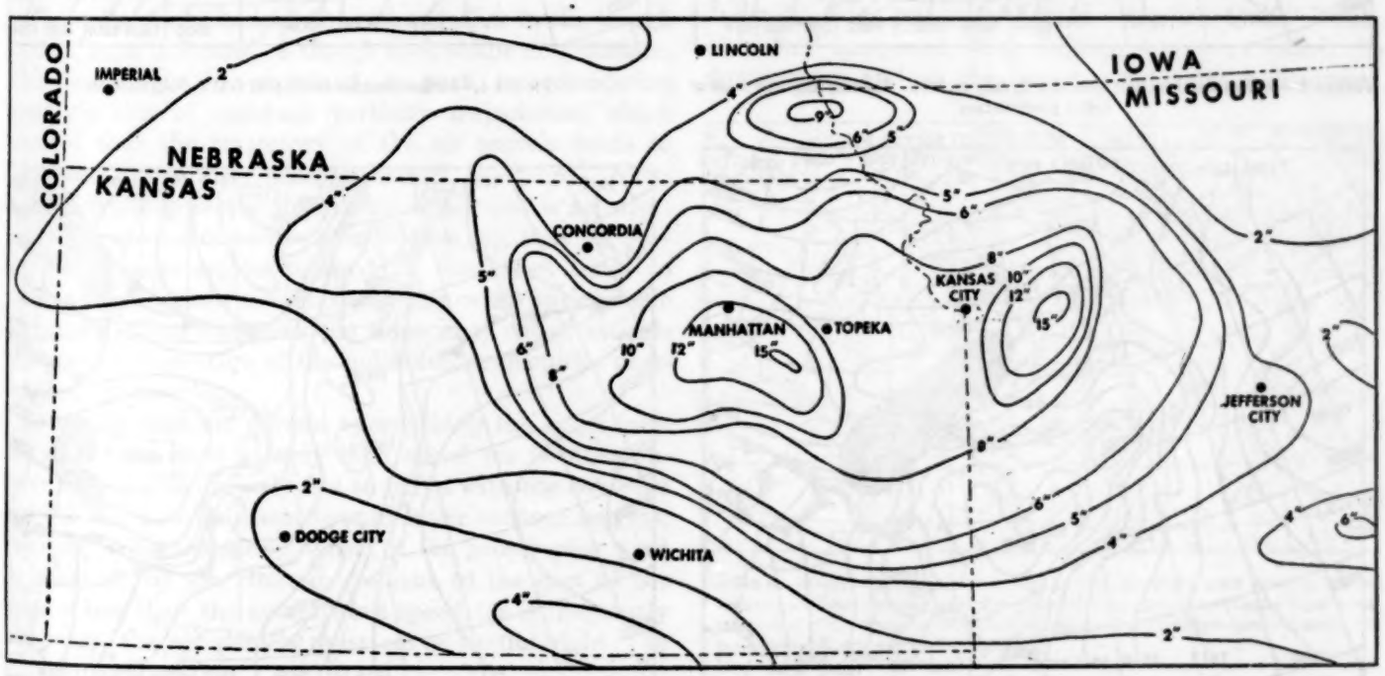

FIGURE 1.—Precipitation (inches) for period July 4–17, 1951. (Based on incomplete preliminary data. Map as drawn by the River Services Section, U. S. Weather Bureau.)

TABLE 2.—*24-hour totals of rainfall (inches) for selected Kansas stations* [2]

Station	July 10	July 11	July 12	July 13	Four-day total
Concordia	0.95	1.28	2.04	----------	4.27
Dodge City	1.98	1.50	.03	.47	3.98
Emporia	1.63	4.60	3.11	1.69	11.03
Goodland	.45	.35	1.69	T	2.49
Harveyville	2.81	4.36	2.67	1.12	10.96
Herrington	2.70	5.50	2.30	.75	11.25
Hill City	.38	2.89	1.95	----------	5.22
Kansas City	.34	1.78	1.38	.68	4.18
Manhattan	4.86	2.48	3.25	.48	11.07
Topeka	.49	2.34	4.00	----------	6.83
Wichita	T	.42	.22	.27	.91

District of Kansas City was 35.86 feet at 0600 local time on the 14th. This is 13.86 feet above bankfull level. The all time high water mark for Kansas City is 38 feet, as gleaned from Indian markers and stories by witnesses to the flood of June 15, 1844 [1]. Bonner Springs, Kans. (southwest of Kansas City, on the Kansas River) had an observed highest stage of 38.9 feet at 2300 local time on the 13th, against a bankfull level of 21 feet [1].

SURFACE CIRCULATION

The series of surface weather maps (figs. 2–5) represents the surface pattern during the period July 10–13. Under the influence of an upper ridge over the Alaskan Gulf the cold fronts moved down the western Plains to Kansas, and then more slowly to Oklahoma where they finally frontolized. The map of July 10 (fig. 2) shows a cold front over southern Kansas which had come into that area on the previous day. By July 11 (fig. 3) it was in the process of "washing out" as a new surge had entered the northwest triangle of the State. This new surge slowed down over Kansas on July 12 (fig. 4) and then moved very

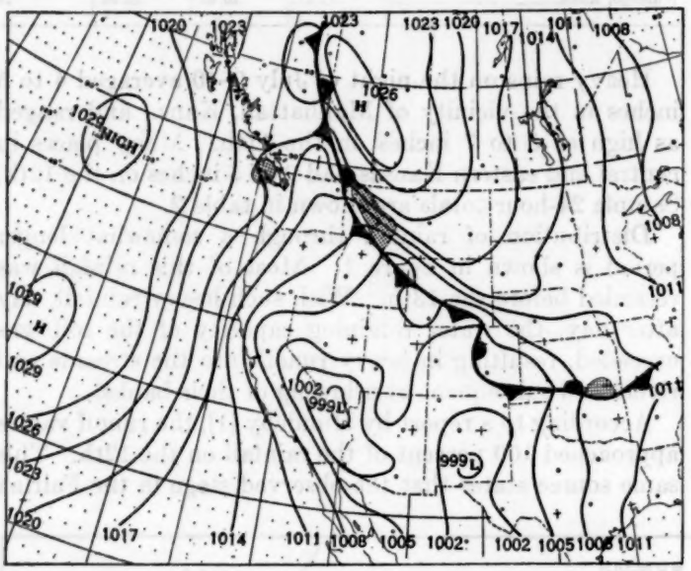

FIGURE 2.—Surface weather chart, 0030 GMT, July 10, 1951. Shading indicates areas of active precipitation.

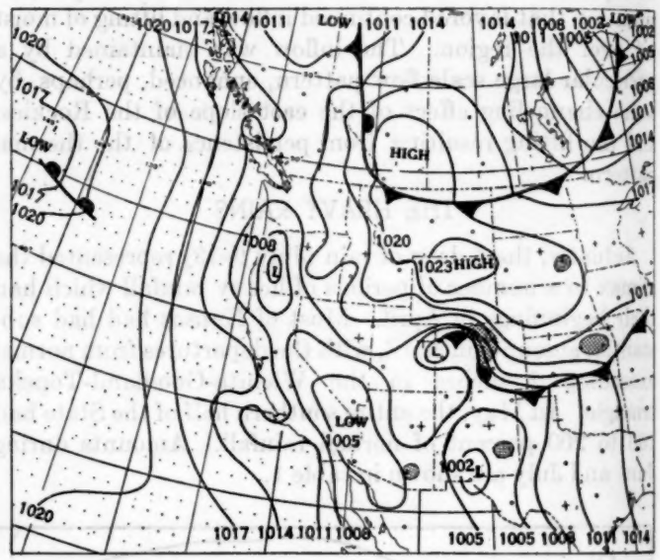

FIGURE 4.—Surface weather chart, 0030 GMT, July 12, 1951.

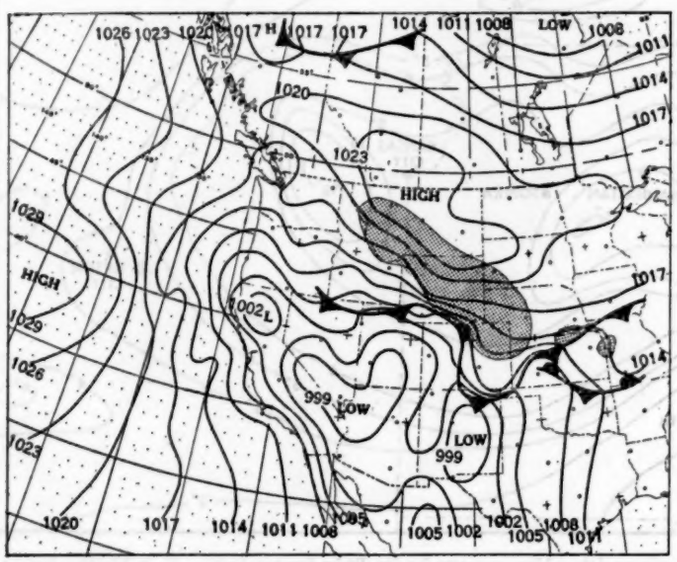

FIGURE 3.—Surface weather chart, 0030 GMT, July 11, 1951.

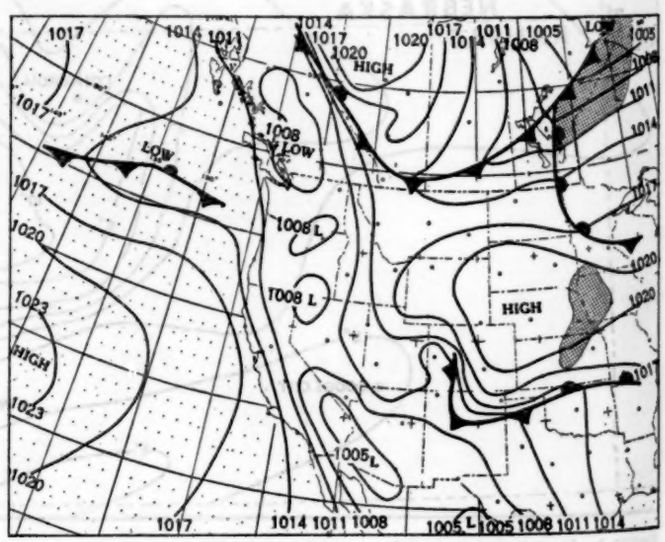

FIGURE 5.—Surface weather chart, 0030 GMT, July 13, 1951.

slowly into northern Oklahoma during the next 24 hours. By July 13 (fig. 5) it had changed its direction of movement and acted as a warm front.

This sequence produced not widespread rains over the Kansas-Oklahoma area, as often occur when cold air masses move in under warm air in that region, but rather, intense local showers and thunderstorms as the convectively unstable air rode up the frontal surface of the Polar air. These downpours occurred mainly during the night and early morning hours, as is typical of summer precipitation in the Middle Plains area. Before investigating the frontal lifting mechanism more closely, it will be helpful to examine the role of the circulation aloft in the surges of cold air.

CIRCULATION ALOFT

A characteristic pattern of the middle troposphere air flow during June and the early part of July consisted of a north-south ridge of high pressure over the Gulf of Alaska and a trough of low pressure extending from the northern Plains southwestward to the southern Plateau. Once this trough was established it persisted for 7 to 10 days at a time. While this pattern prevailed heavy rain fell over Kansas.

This ridge-trough pattern was accompanied by intermittent surges of Polar air into the northern Plains States. These masses of cold air moved southward along the eastern shoulders of the Rocky Mountains, displacing or blocking the northward flow of moist tropical maritime air from the Gulf of Mexico. The southward movement of cold air was associated with the circulation around the upper level ridge, while the northward flow of warm air was supported by the flow on the eastern side of the upper level trough.

The ridge might be looked upon as father to the trough in that, once it formed, a trough took shape downstream. This fact might be explained, in part, by considering Rossby's idea of constant vorticity trajectories, which requires that the trajectory of the air parcels tends to curve southward after passing through the ridge. However, a dynamic factor that seems important is an effect which has been pointed out by Wobus [3]; that is, particularly in the region referred to, the ridge tends to develop and remain nearly stationary with anticyclonic curvature (along and near the ridge line) which exceeds any possible curvature of the individual trajectories passing through the ridge.

Assuming that air parcels approaching the ridge from the southwest have a fairly high speed (as is often observed) they will not only fail to curve with the contours but will move across them toward lower contour heights, resulting in acceleration. Then, if the geostrophic wind as indicated by the contour gradient to the east of the ridge is less than the actual wind speed (as is frequently observed), the air parcels must curve to the right. In doing so they move toward higher contours, decelerate, and later recurve to the left, the trajectory taking the form of a trough.

It was also shown by Wobus [3] that the magnitude of this effect is such as to form a trough of the dimensions observed, as for example, over the plateau when there is a stationary ridge over western Canada. His theory assumes that the contour field tends eventually to become adjusted to the wind flow, requiring for the formation of the trough that the atmosphere undergo net horizontal mass divergence in the area of trough formation. This in turn requires that the total horizontal divergence which presumably occurs mostly in the middle troposphere, exceed the total convergence at other levels. These requirements seem to be met when winds in the middle and upper troposphere are relatively strong, particularly as a new surge of stronger winds moves into and through the stationary ridge.

These effects seem to have been important during the period of recurring flood rains, when northeast-southwest troughs formed from time to time and moved only slowly across the northern Plains and Plateau areas. While conditions to the northward and northwestward are not shown completely on the accompanying charts, some evidence of the effect may be seen by comparing figures 6 and 7. In figure 6, the 700-mb. chart for July 9, there is a rather weak east-west trough across Washington and northern Montana. Figure 7, the 700-mb. chart 24 hours later, shows easterly winds over Washington. These winds could only have originated in the ridge to the north, and were accompanied by an east-west trough within which a developing low pressure center was forming over southeastern Idaho.

From time to time during June and the first half of July, the ridge would split in the Alaskan Gulf. Whenever this happened, new adjustments were called for downstream and so the trough would either disappear,

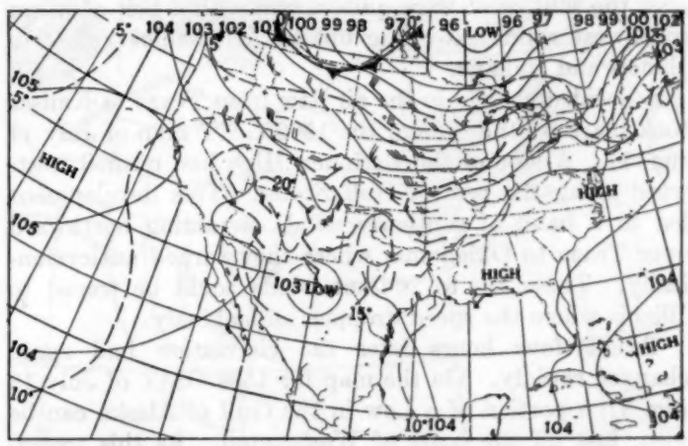

FIGURE 6.—700-mb. chart, 0300 GMT, July 9, 1951. Contours (solid lines) at 100-foot intervals are labeled in hundreds of geopotential feet. Isotherms (dashed lines) are at intervals of 5° C. Barbs on wind shafts are for speed in knots (pennant=50 knots, full barb=10 knots, and half barb=5 knots).

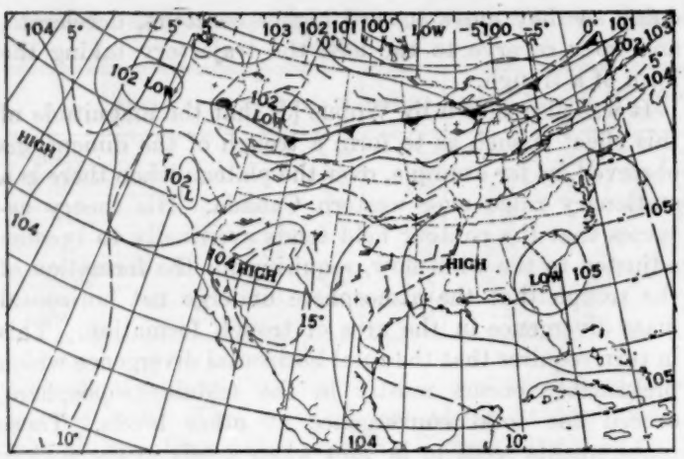

FIGURE 7.—700-mb. chart, 1500 GMT, July 11, 1951.

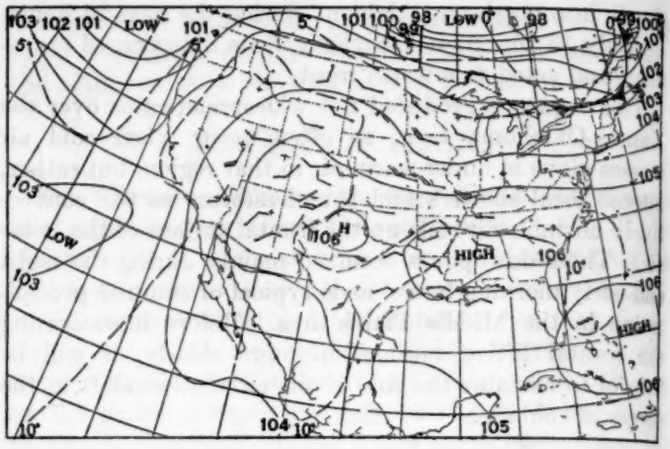

FIGURE 8.—700-mb. chart, 1500 GMT, July 13, 1951.

move bodily, or re-form elsewhere. Such disruption took place July 13, when the rains ceased and the more normal summer weather returned to Kansas. The changes in the circulation aloft during the heavy rain period are examined in more detail in the next section by reference to 700-mb. charts. A fuller discussion of the changing pattern of the general circulation and the associated surface effects is covered elsewhere in this issue by Oliver [4] and in a previous issue of the Review by Clem [5].

700-MB CIRCULATION

Three maps serve to illustrate the circulation at the 700-mb. level during the period of heavy rain. The 0300 GMT map of July 9 (fig. 6) shows the Kansas area under a stream of downslope northwest winds with only a small area of cold air advection in extreme northeast Kansas. Along both coast lines of the United States, and generally south of 40° N. latitude, ridge conditions predominated. A connecting ridge of high pressure stretched across the southern tier of States. Temperatures aloft over the southwest were quite warm with a belt of warm southwest winds extending up the Mississippi Valley to Illinois and Indiana.

A decided change in the air flow from Texas to Kansas took place by the time of the 1500 GMT map of July 11 (fig. 7). A lobe of the Bermuda High had pushed westward along the central Gulf States. This development led to a band of southerly winds streaming northward over Texas to Oklahoma, where they turned anticyclonically. These 15- to 20-knot winds could be traced to Illinois where the speed dropped off suddenly.

Twenty-four hours later the circulation had again changed rapidly. On the map for 1500 GMT of July 13 (fig. 8), a portion of a Low in the Gulf of Alaska can be seen, just off the coast of Washington. As this trough developed in strength and area the ridge downstream from it underwent readjustment. On this map a ridge extended in a southeast to northwest direction from Texas to Idaho. As the heights rose over Texas, the southerly winds from the Gulf of Mexico were cut off. All that can be seen of the mass of warm air is a narrow band of high temperatures extending from Del Rio, Tex., to near Memphis, Tenn.

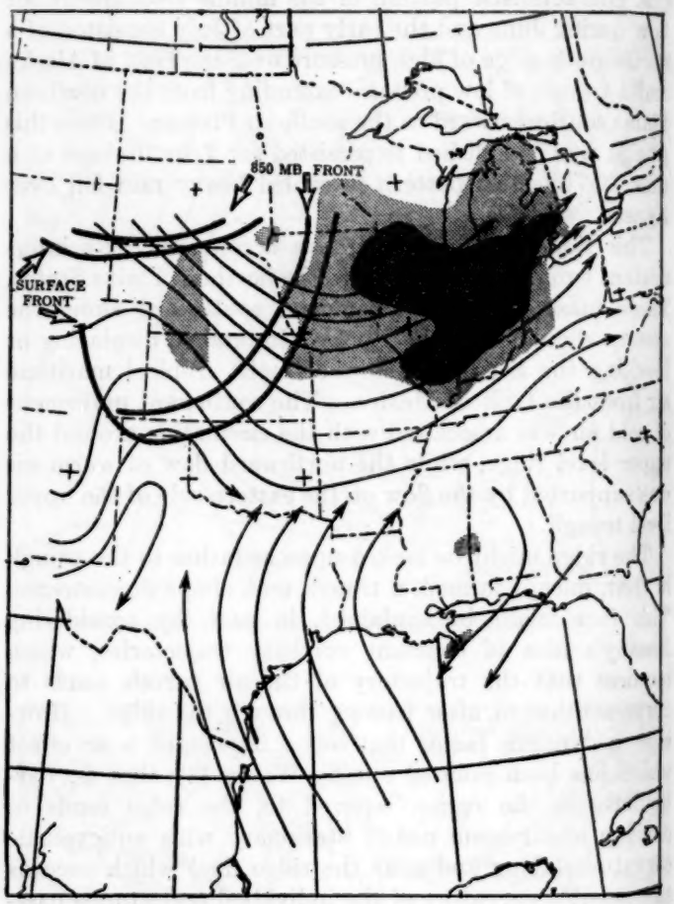

FIGURE 9.—Streamline-rainfall chart, 0300 GMT, July 9, 1951. Streamlines (solid lines) of instantaneous wind direction at 700 mb. Shading indicates areas of rainfall during the 24 hours ending 1230 GMT, July 9, 1951. (Light shading: trace to less than 0.5 inch; dark shading: 0.5 inch or greater.) Surface and 850-mb. fronts (heavy solid lines) are appropriately labeled.

FRONTAL LIFTING

In order to see how the frontal lifting mechanism worked in the lower troposphere, the weather may be examined in terms of the flow pattern aloft as indicated by the streamlines of instantaneous wind direction at 700 mb., the positions of the surface and 850-mb. fronts, and the reported rainfall areas and amounts. The resulting series of maps (figs. 9–11) shows the relationship between all these elements.

On the map for 0300 GMT July 9 (fig. 9), rainfall is shown in a small area east of Goodland, Kans., and in the Kansas City area. In both areas the rain occurred with thunderstorms prior to midnight of July 8. The broad area of heavy rainfall over the Illinois region occurred with a squall line in the deep layer of moist, unstable air. The rains in Kansas occurred only in relation to the frontal passage and amounts were light (less than 0.25 inch).

The air flow, as depicted by the arrows, was in two broad streams. The first moved downslope over the top of the cold dome in northwest Kansas. The second moved up from Texas, its northern boundary being just north of the Red River Valley of Oklahoma. This air was maritime-tropical in type and convectively unstable aloft. Its surface temperatures ranged from low to middle eighties, and dew points from 70° to 75° F. In the confluence zone, where the two major air streams met over eastern Oklahoma and Arkansas, no rain fell during the 24 hours because lifting, if any, was insufficient. Over Kansas, no rains of consequence developed because of the prevalence of downslope flow.

In the 24 hours ending at 1500 GMT, July 11 (fig. 10), the picture changed rapidly as heavy rains developed over Kansas and Missouri. Just west of Topeka, amounts were as high as 4.5 inches. The zone of Gulf air extended all the way from Texas to Illinois. The southern limit of the heavy rains coincided rather closely with the surface cold front. Where the air stream was intercepted by the leading edge of the cold air dome, heavy falls of rain took place, as can be seen by the shaded areas on the map. By tracing the path of the moist winds it is rather clearly indicated that frontal lifting was the action which produced the heavy rainfall. Only light showers had fallen along the Gulf coast of Texas, and from there to the front no rain was reported.

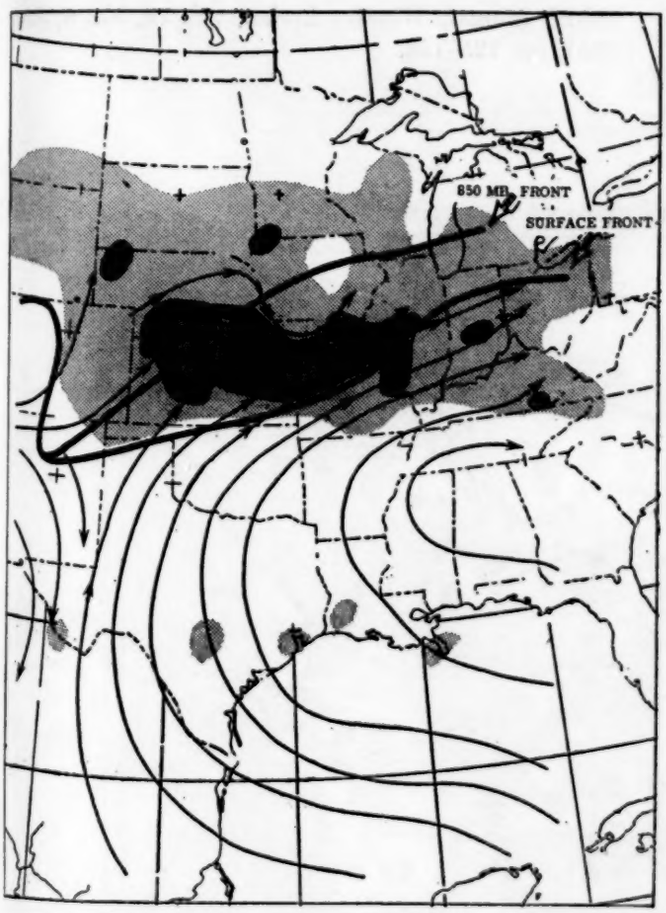

FIGURE 10.—Streamline-rainfall chart, 1500 GMT, July 11, 1951. Shading indicates areas of rainfall during the 24 hours ending 1230 GMT, July 12, 1951.

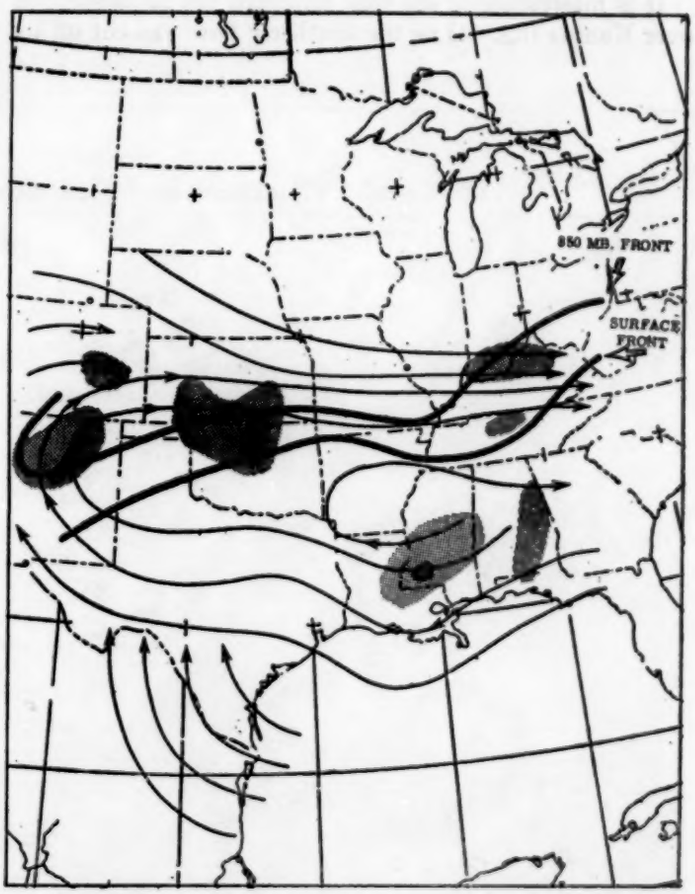

FIGURE 11.—Streamline-rainfall chart, 1500 GMT, July 13, 1951. Shading indicates areas of rainfall during the 24 hours ending 1230 GMT, July 14, 1951.

The sounding for San Antonio, Tex., showed moist air to just above 700 mb. with a rapid drop-off in moisture content above that level. At the same time, the air above Oklahoma City was just as moist to about the same level, but at higher levels was even dryer than over San Antonio. In other words, unstable air moved long distances with a high potential for rain which was realized only when subjected to frontal lifting.

The sounding at Albuquerque indicated very dry air from the surface to about 600 mb. which, together with the fact that the flow in that region was anticyclonic, suggests that this air was subsiding.

On the map for 1500 GMT, July 13 (fig. 11), the belt of southerly winds is found mostly below 36° N. latitude. The San Antonio sounding, in the tropical air, is more moist than the day before. All that remained of the moisture band at Oklahoma City was a sharply defined layer some 30 millibars thick at 700 mb. Over the Kansas region the winds were once again from a westerly direction and essentially downslope. Although the front moved on to Oklahoma, only a small rain area had developed and the amounts were less than .25 inch. Rains in the Enid to Oklahoma City zone were the result of thunderstorms in the evening of July 12.

It is interesting to see that although the rains stopped over Kansas (fig. 11) as the southerly flow was cut off by the downslope motion and rearrangement of the flow pattern, the eastern portion of New Mexico showed thunderstorm rains exceeding one inch where the southeast winds, moving upslope, were further lifted by the advancing cold front.

REFERENCES

1. Gordon Hundeby, Report on the Great Flood of July 1951 on the Kansas and Missouri Rivers at Kansas City, U. S. Weather Bureau Airport Station, Kansas City, Mo., August 1951. (In cooperation with Weather Bureau Area Hydrologic Engineer and River Forecast Center.) (Unpublished.)
2. U. S. Weather Bureau, *Climatological Data, Kansas*, vol. LXV, No. 7, July 1951.
3. H. B. Wobus, "A Systematic Method of Wind Forecasting at 500 mb.," paper presented at 98th National Meeting of American Meteorological Society, Washington, D. C., April 20–22, 1948. (Unpublished.)
4. V. J. Oliver, "The Weather and Circulation of July 1951," *Monthly Weather Review*, vol. 79, No. 7, July 1951, pp. 143–146.
5. L. H. Clem, "The Weather and Circulation of June 1951," *Monthly Weather Review*, vol. 79, No. 6, June 1951, pp. 125–128.

U. S. GOVERNMENT PRINTING OFFICE: 1951

Chart I. A. Average Temperature (°F.) at Surface, July 1951.

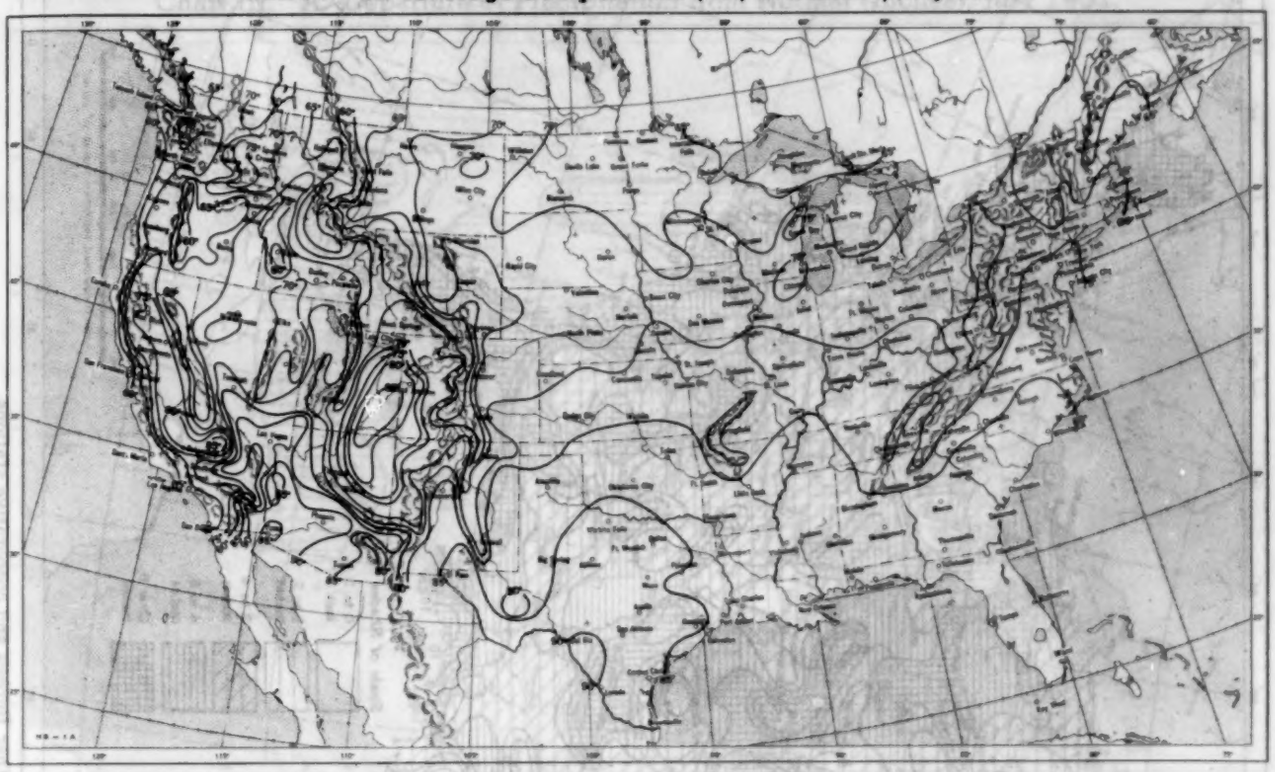

B. Departure of Average Temperature from Normal (°F.), July 1951.

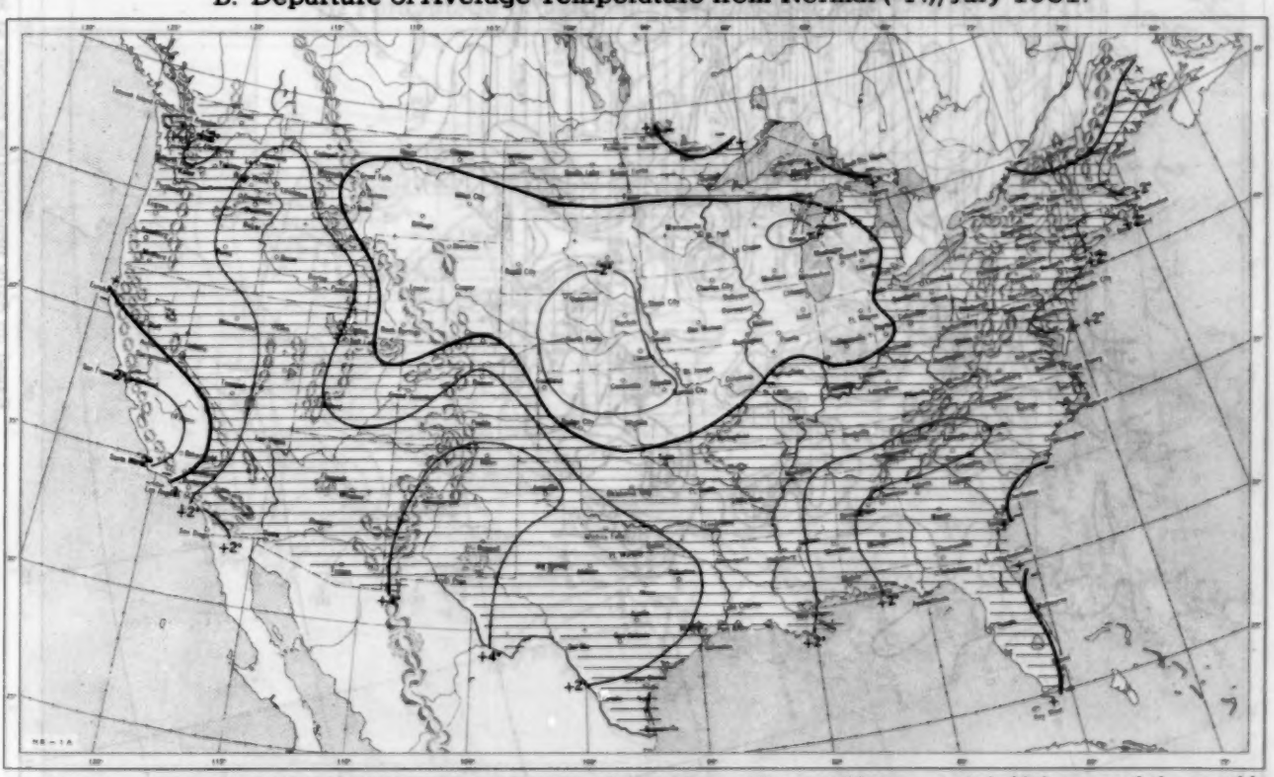

A. Based on reports from 800 Weather Bureau and cooperative stations. The monthly average is half the sum of the monthly average maximum and monthly average minimum, which are the average of the daily maxima and daily minima, respectively.
B. Normal average monthly temperatures are computed for Weather Bureau stations having at least 10 years of record.

Chart II. Total Precipitation (Inches), July 1951.

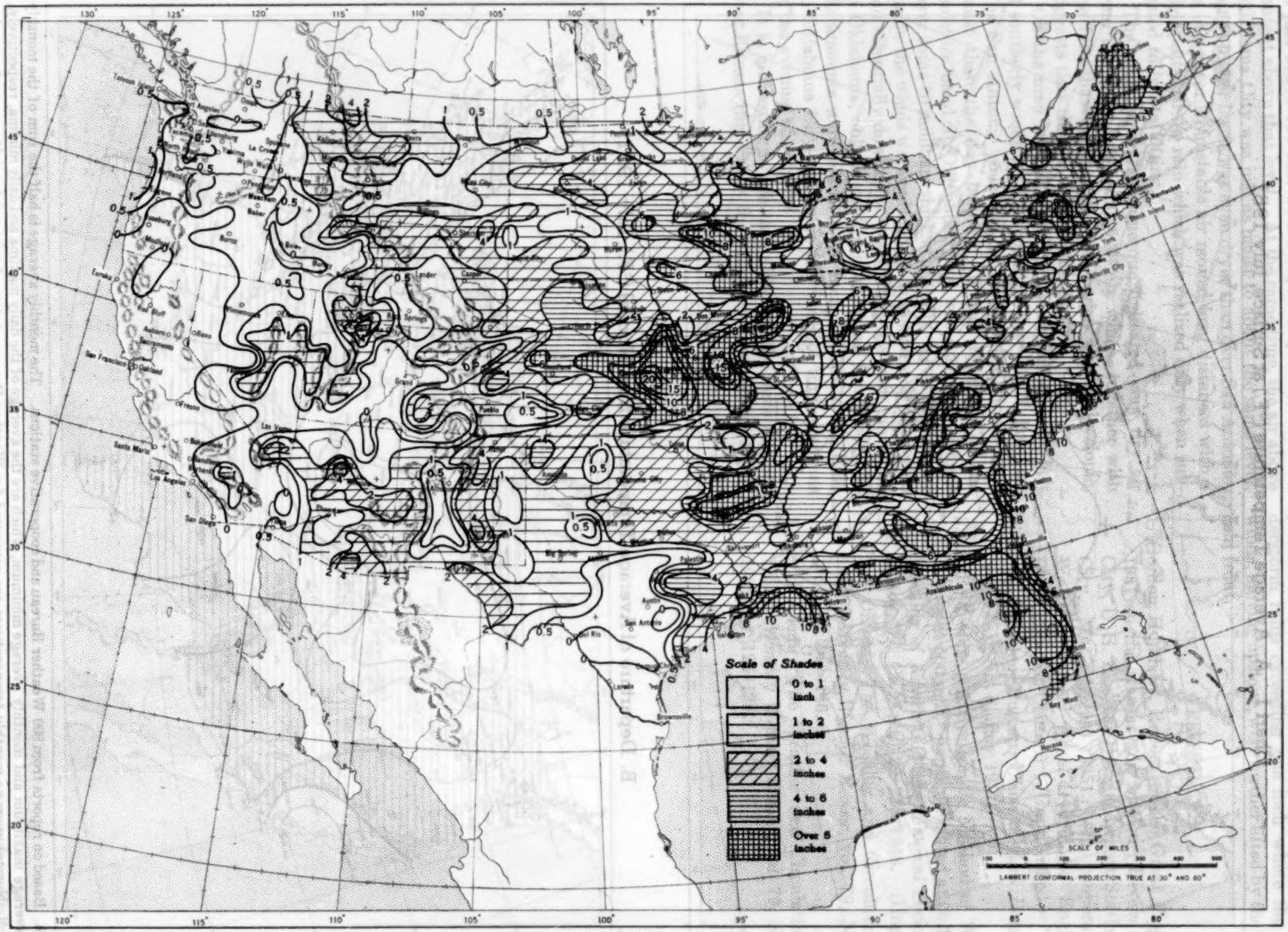

Based on daily precipitation records at 800 Weather Bureau and cooperative stations.

Chart III. A. Departure of Precipitation from Normal (Inches), July 1951.

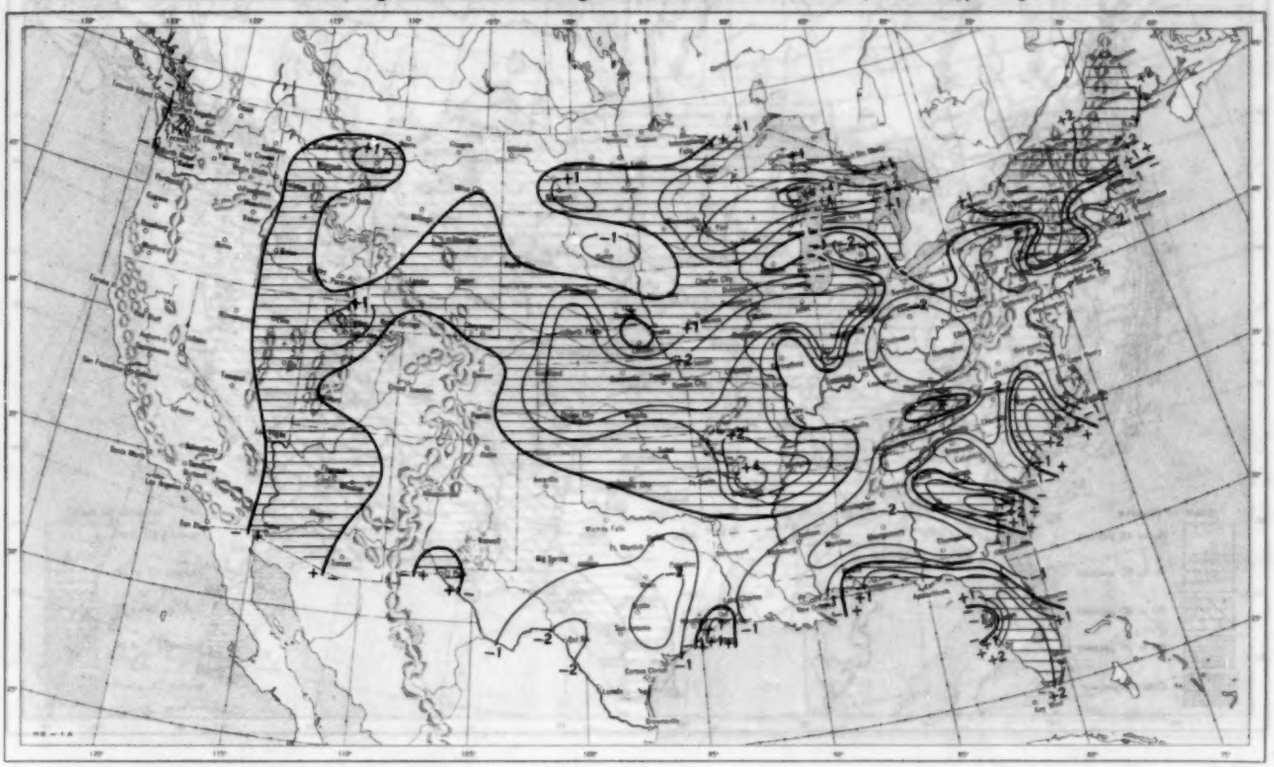

B. Percentage of Normal Precipitation, July 1951.

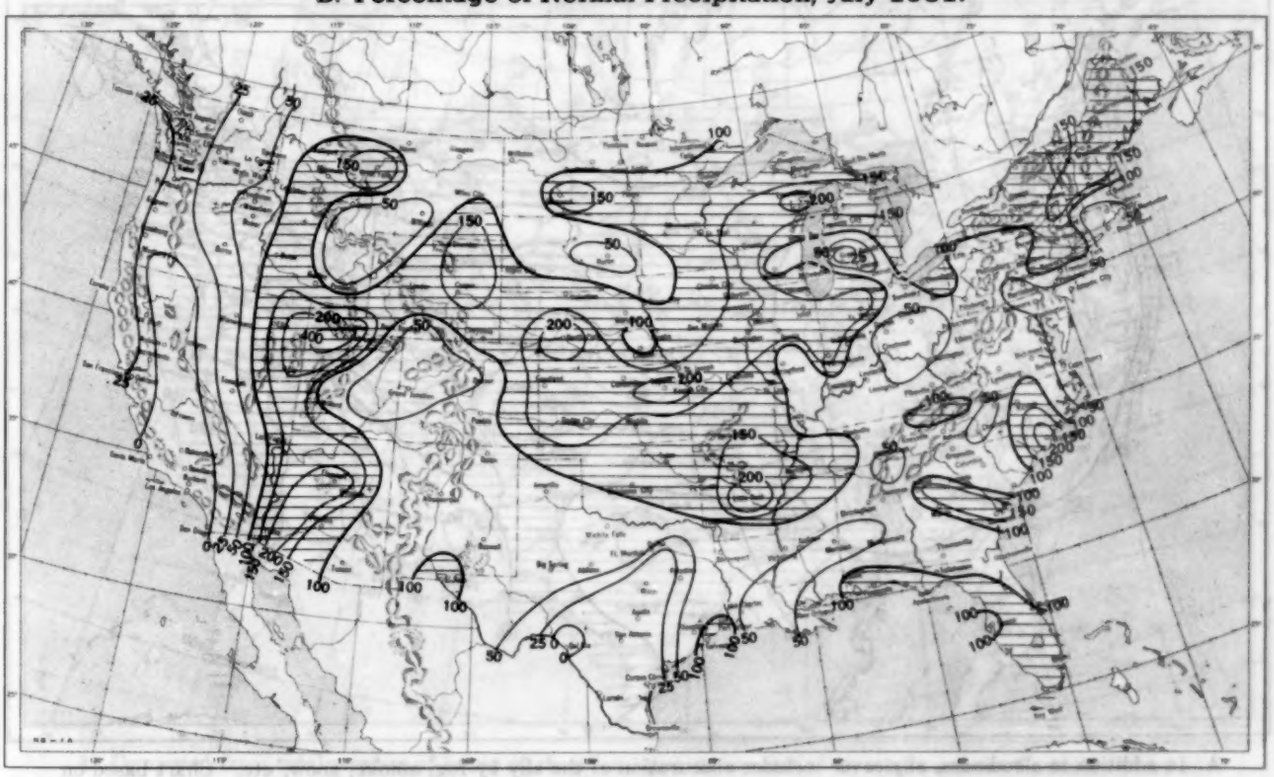

Normal monthly precipitation amounts are computed for stations having at least 10 years of record.

Chart VI. A. Percentage of Sky Cover Between Sunrise and Sunset, July 1951.

B. Percentage of Normal Sky Cover Between Sunrise and Sunset, July 1951.

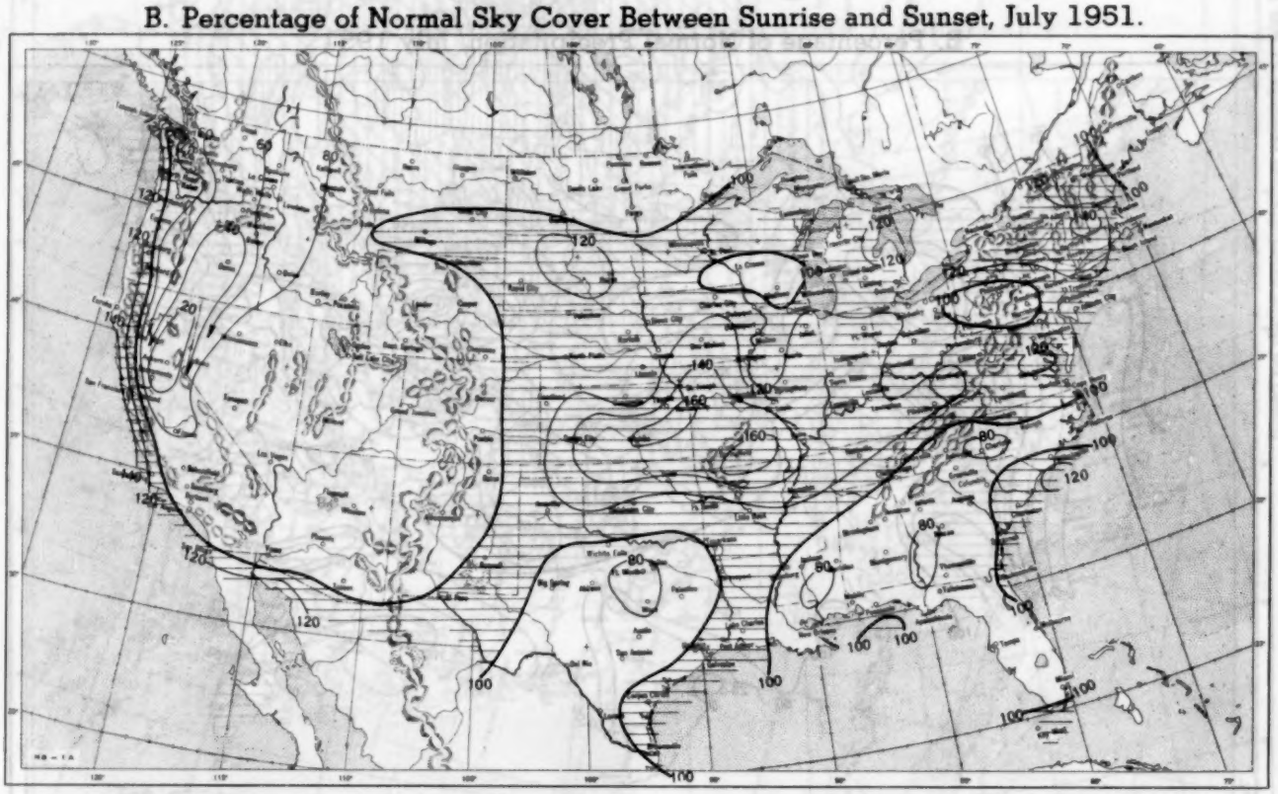

A. In addition to cloudiness, sky cover includes obscuration of the sky by fog, smoke, snow, etc. Chart based on visual observations made hourly at Weather Bureau stations and averaged over the month. B. Computations of normal amount of sky cover are made for stations having at least 10 years of record.

Chart VII. A. Percentage of Possible Sunshine, July 1951.

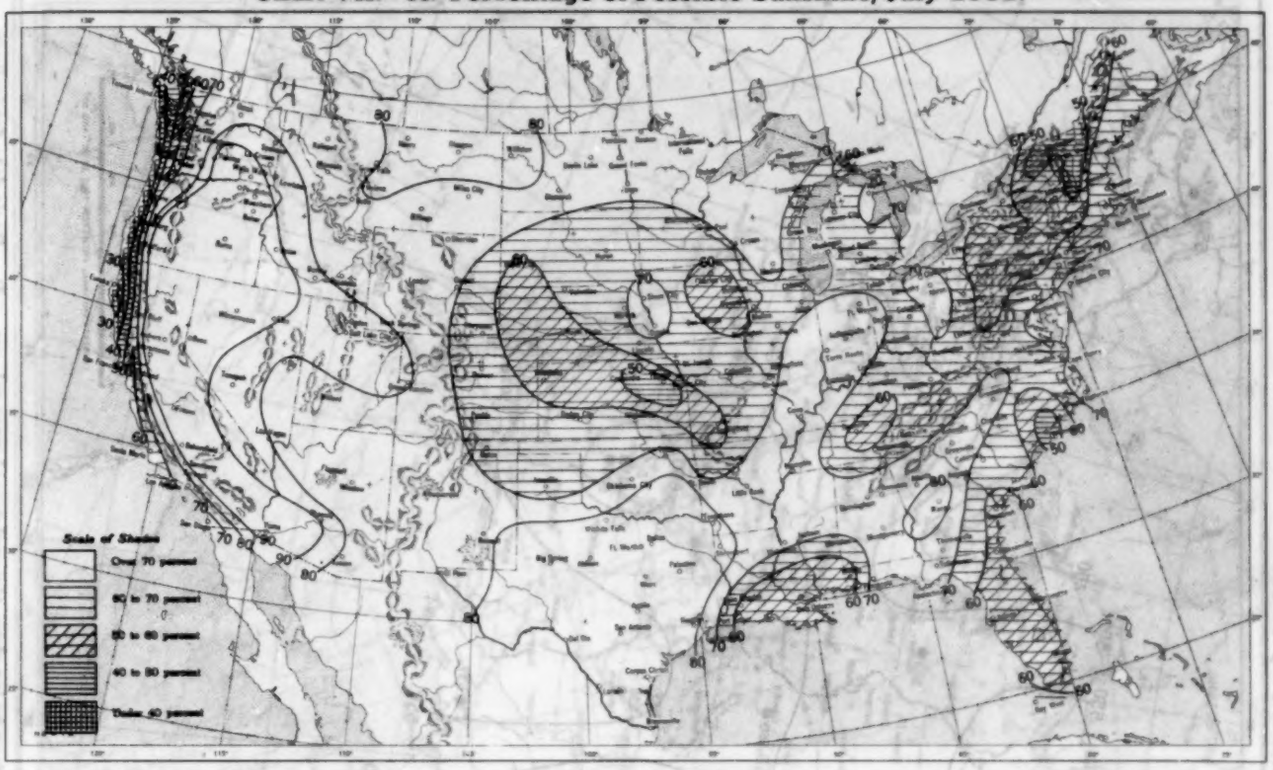

B. Percentage of Normal Sunshine, July 1951.

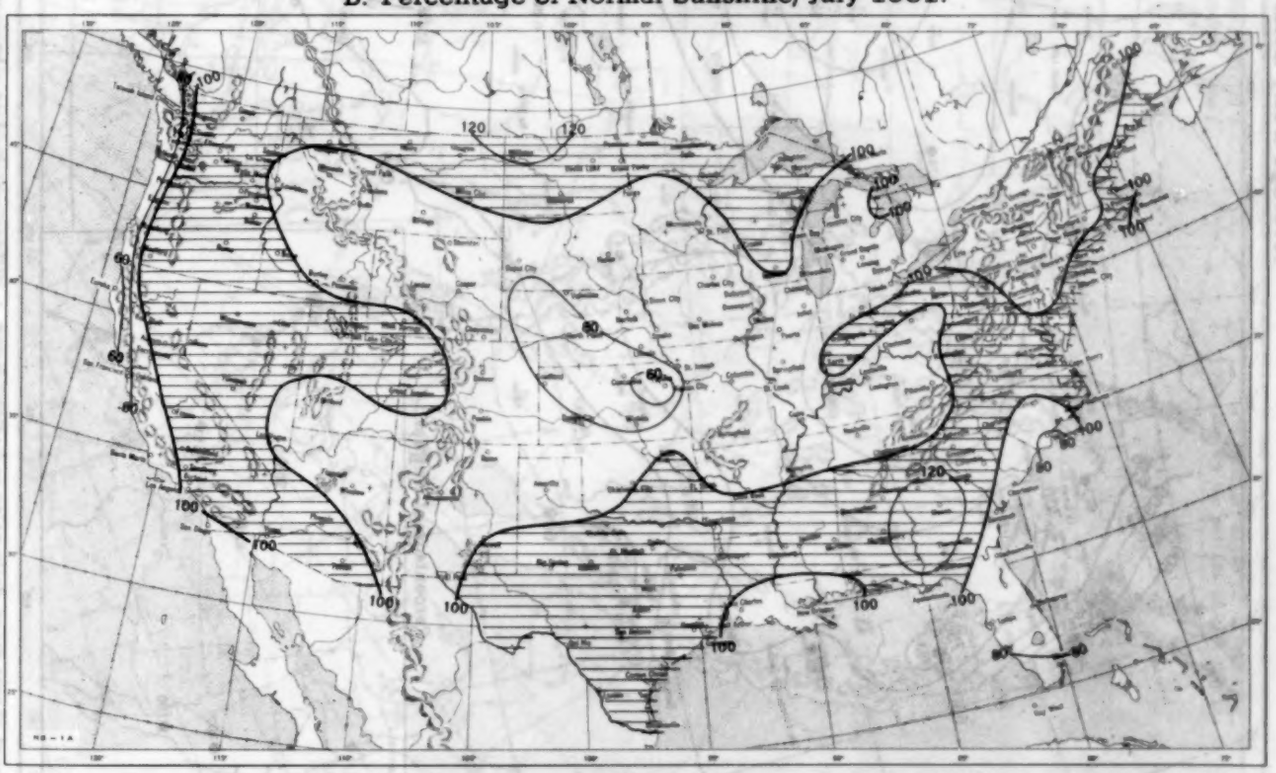

A. Computed from total number of hours of observed sunshine in relation to total number of possible hours of sunshine during month. B. Normals are computed for stations having at least 10 years of record.

Chart VIII. Average Daily Values of Solar Radiation, Direct + Diffuse, July 1951. Inset: Percentage of Normal Average Daily Solar Radiation, July 1951.

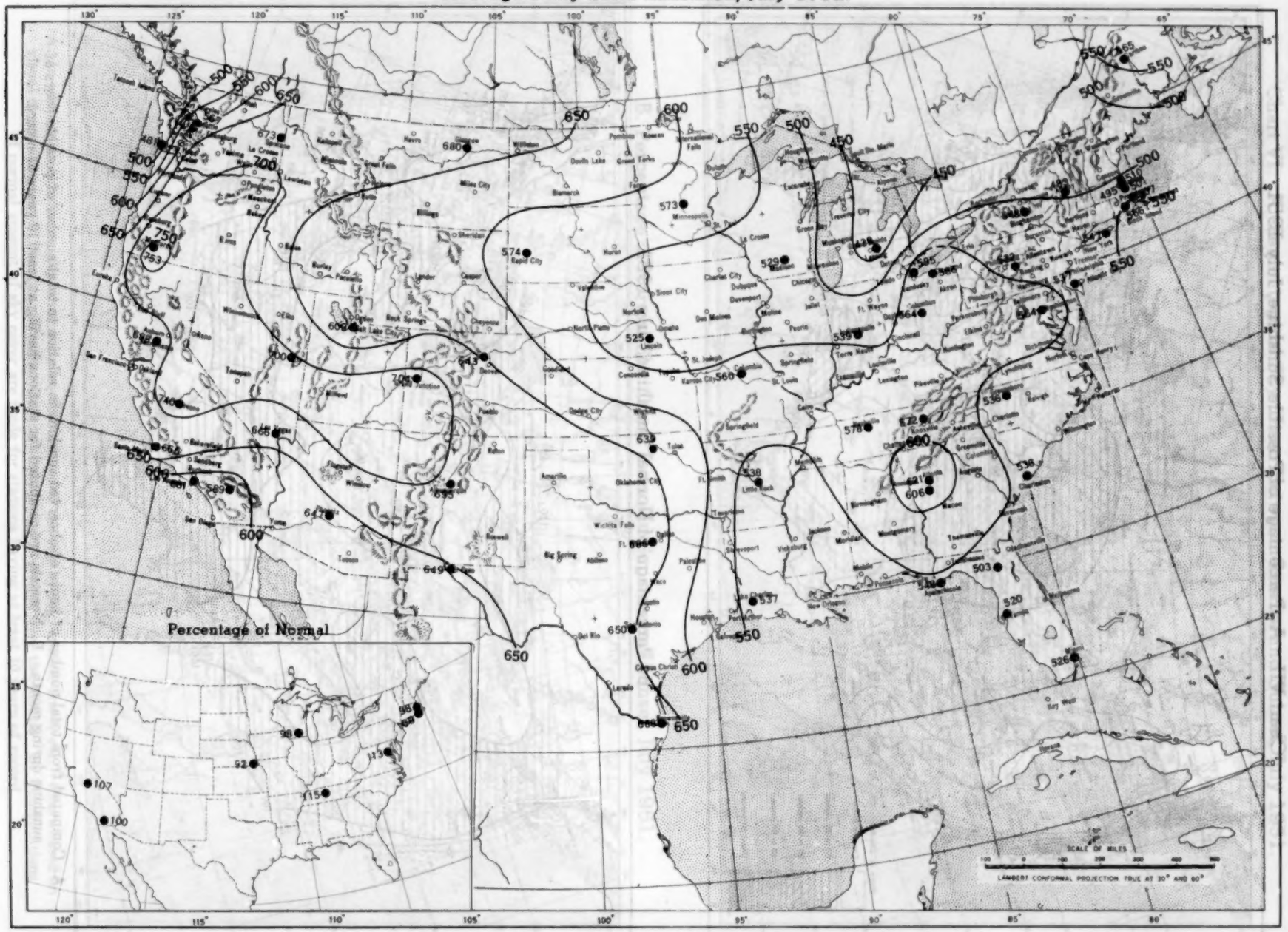

Chart shows mean daily solar radiation, direct + diffuse, received on a horizontal surface in langleys (1 langley = 1 gm. cal. cm. $^{-2}$). Basic data for isolines are shown on chart. Further estimates obtained from supplementary data for which limits of accuracy are wider than for those data shown. Normals are computed for stations having at least 9 years of record.

Computed for stations having at least 9 years of record.

Chart IX. Tracks of Centers of Anticyclones at Sea Level, July 1951

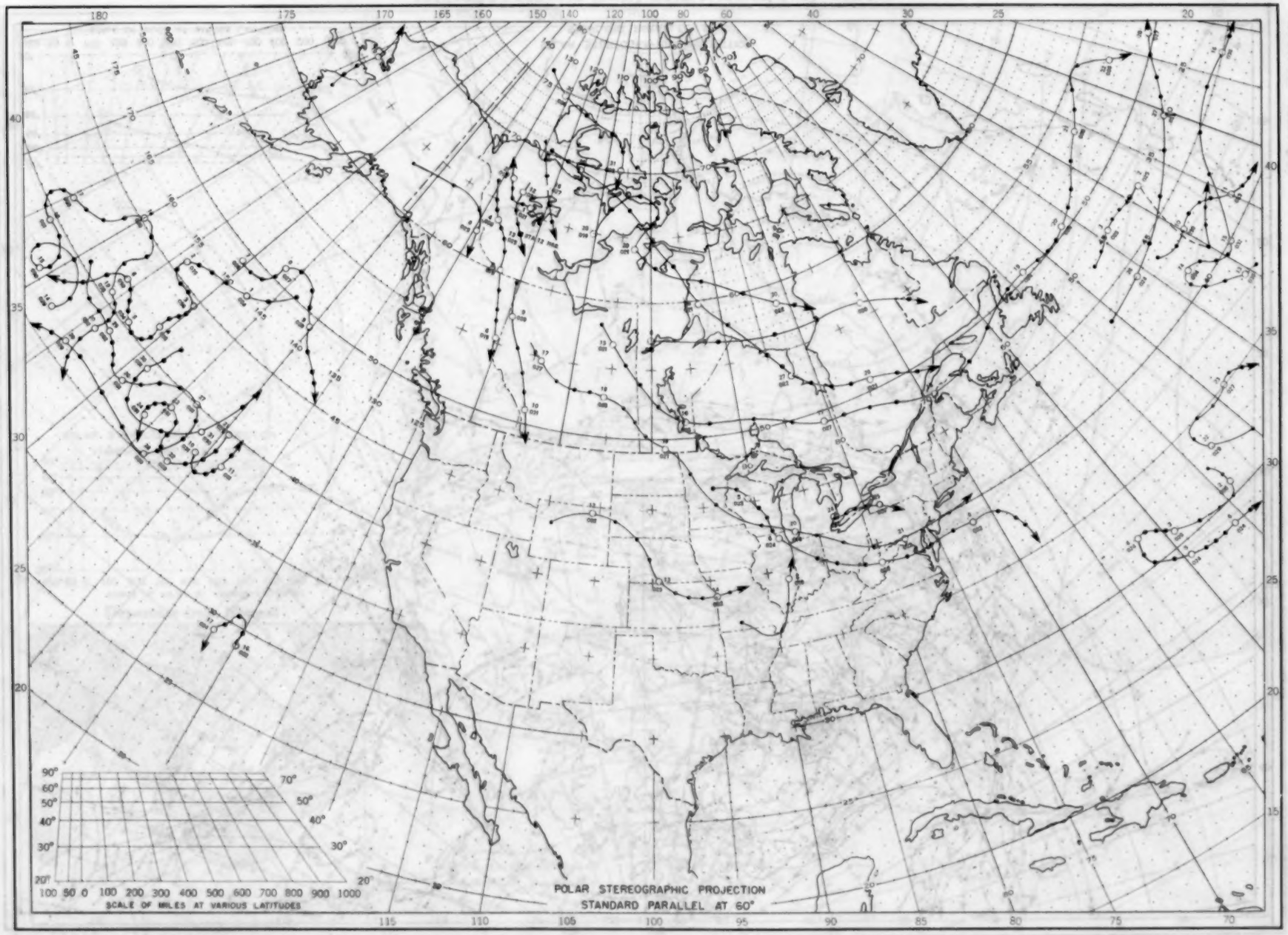

Circle indicates position of center at 7:30 a. m. E. S. T. Figure above circle indicates date, figure below, pressure to nearest millibar. Dots indicate intervening 6-hourly positions. Squares indicate position of stationary center for period shown. Dashed line in track indicates reformation at new position. Only those centers which could be identified for 24 hours or more are included.

Chart X. Tracks of Centers of Cyclones at Sea Level, July 1951.

Circle indicates position of center at 7:30 a. m. E. S. T. See Chart IX for explanation of symbols.

Chart XI. Average Sea Level Pressure (mb.) and Surface Windroses, July 1951. Inset: Departure of Average Pressure (mb.) from Normal, July 1951.

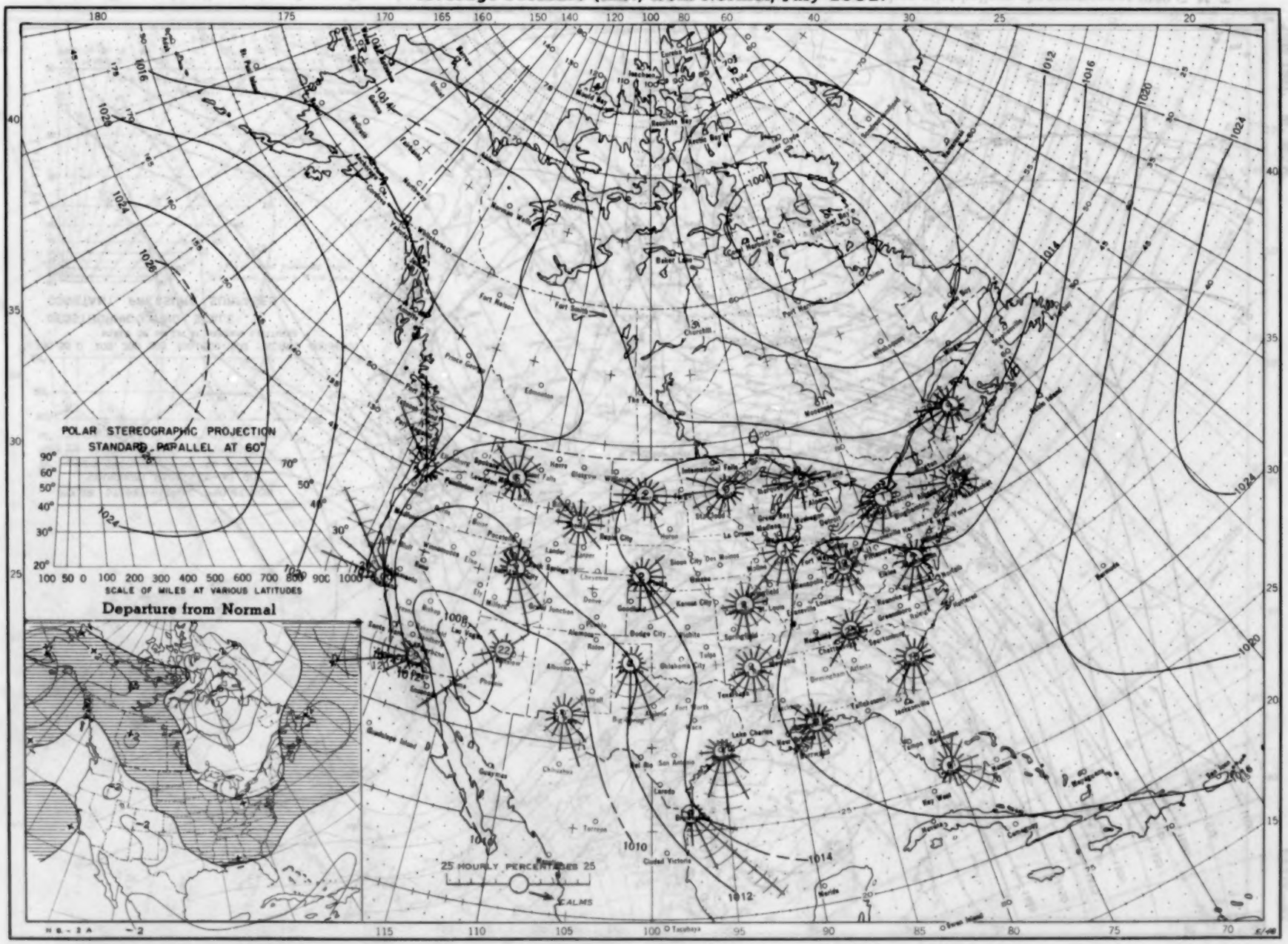

Average sea level pressures are obtained from the averages of the 7:30 a. m. and 7:30 p. m. E. S. T. readings. Windroses show percentage of time wind blew from 16 compass points or was calm during the month. Pressure normals are computed for stations having at least 10 years of record and for 10° intersections in a diamond grid from map readings for 20 years of the Historical Weather Maps, 1899–1939.

Chart XII. Average Dynamic Height in Geopotential Meters (1 g.p.m. = 0.98 dynamic meters) of the 850-mb. Pressure Surface, Average Temperature in °C. at 850 mb., and Resultant Winds at 1500 Meters (m.s.l.), July 1951.

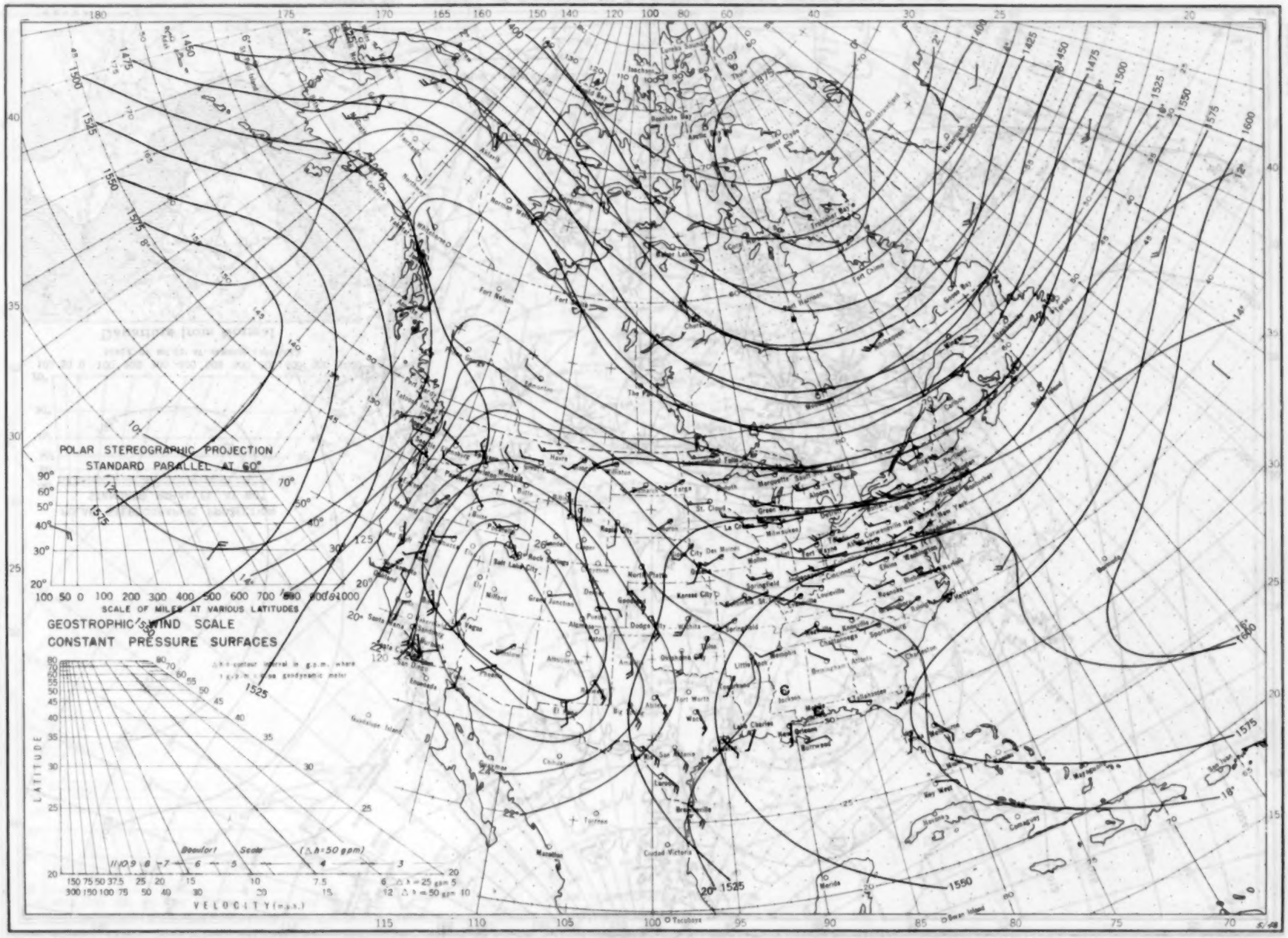

Contour lines and isotherms based on radiosonde observations at 0300 G. M. T. Winds shown in black are based on pilot balloon observations at 2100 G. M. T.; those shown in red are based on rawins taken at 0300 G. M. T.

Chart XIII. Average Dynamic Height in Geopotential Meters (1 g.p.m.. = 0.98 dynamic meters) of the 700-mb. Pressure Surface, Average Temperature in °C. at 700 mb., and Resultant Winds at 3000 Meters (m.s.l.), July 1951.

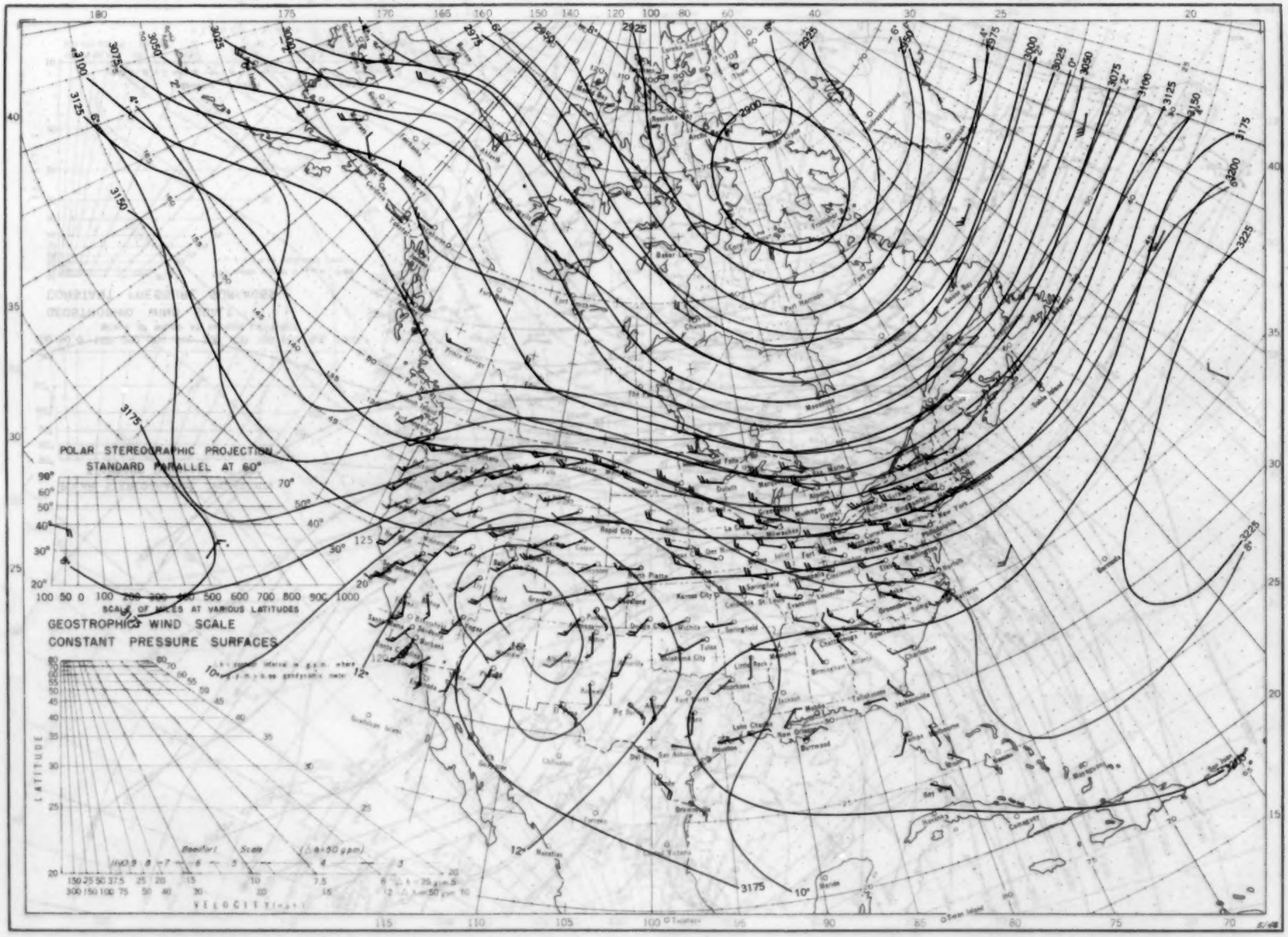

Contour lines and isotherms based on radiosonde observations at 0300 G. M. T. Winds shown in black are based on pilot balloon observations at 2100 G. M. T.; those shown in red are based on rawins taken at 0300 G. M. T.

Chart XIV. Average Dynamic Height in Geopotential Meters (1 g.p.m. = 0.98 dynamic meters) of the 500-mb. Pressure Surface, Average Temperature in °C at 500 mb., and Resultant Winds at 5000 Meters (m.s.l.), July 1951.

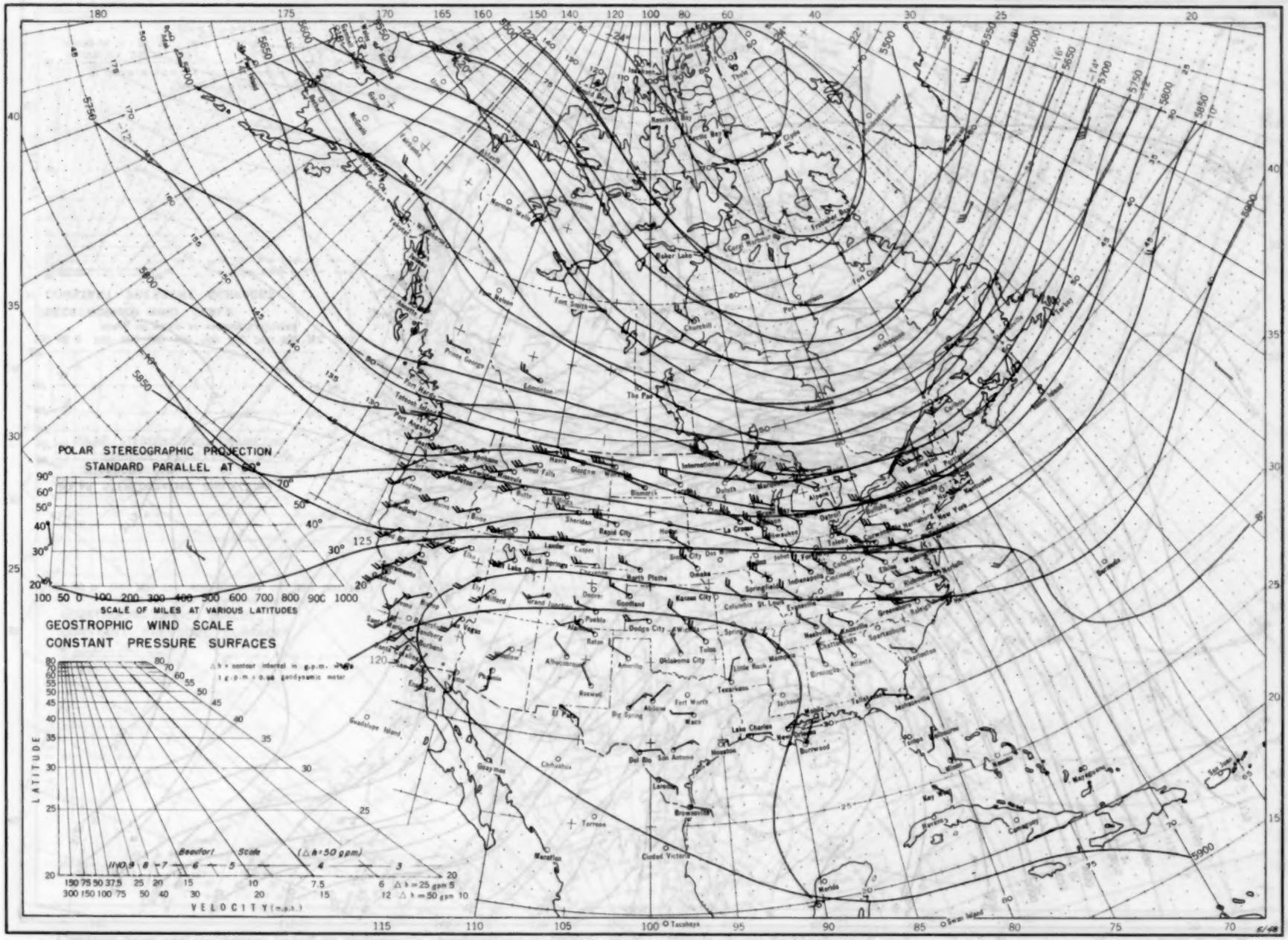

Contour lines and isotherms based on radiosonde observations at 0300 G. M. T. Winds shown in black are based on pilot balloon observations at 2100 G. M. T.; those shown in red are based on rawins at 0300 G. M. T.

Chart XV. Average Dynamic Height in Geopotential Meters (1 g.p.m. = 0.98 dynamic meters) of the 300-mb. Pressure Surface, Average Temperature in °C. at 300 mb., and Resultant Winds at 10,000 Meters (m.s.l.), July 1951.

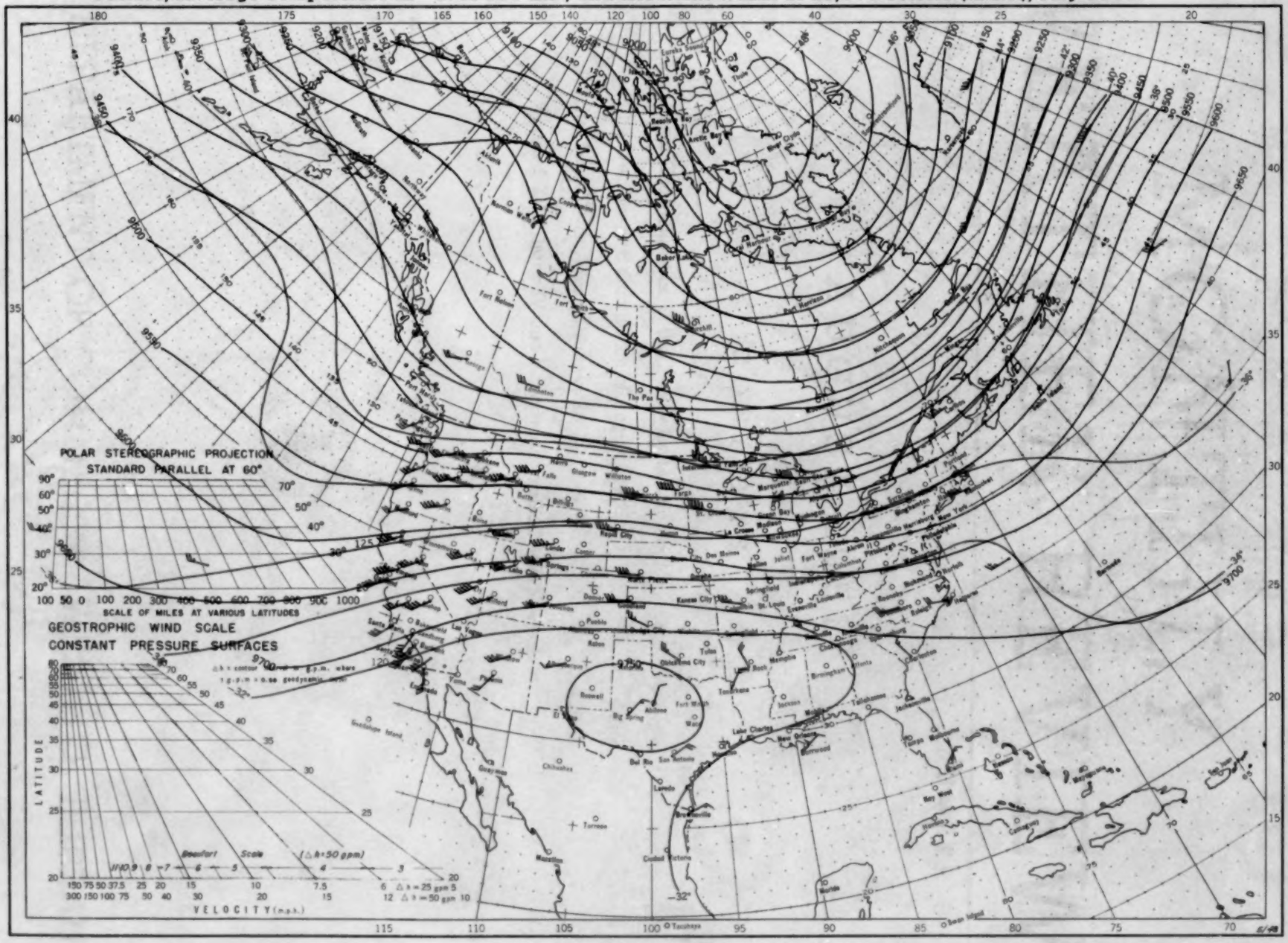

Contour lines and isotherms based on radiosonde observations at 0300 G. M. T. Winds shown in black are based on pilot balloon observations at 2100 G. M. T.; those shown in red are based on rawins at 0300 G. M. T.